INSTRUMENTATION FOR I-V DERIVATIVE MEASUREMENTS OF SEMICONDUCTOR DEVICES

By

K. K. KHURANA

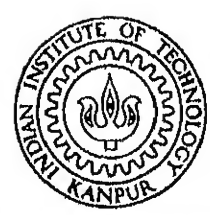

DEPARTMENT OF ELECTRICAL ENGINEERING
INDIAN INSTITUTE OF TECHNOLOGY, KANPUR
JANUARY, 1978

INSTRUMENTATION FOR I-V DERIVATIVE MEASUREMENTS OF SEMICONDUCTOR DEVICES

A Thesis Submitted
in Partial Fulfilment of the Requirements
for the Degree of
MASTER OF TECHNOLOGY

By
K. K. KHURANA

to the
DEPARTMENT OF ELECTRICAL ENGINEERING
INDIAN INSTITUTE OF TECHNOLOGY, KANPUR
JANUARY, 1978

EE-1978-M-KHU-JNS

TO MY GURU

VISHWANATH JI

CERTIFICATE

This is to certify that the thesis entitled, 'Instrumentation for I-V Derivative Measurements of Semiconductor Devices', by K.K.Khurana is a record of work carried out under our supervision and has not been submitted elsewhere for a degree.

(Dr. R.N. Biswas)
Professor

(Dr. R. Sharan)
Professor

Department of Electrical Engineering
Indian Institute of Technology
Kanpur

January, 1978

14.2.78

ACKNOWLEDGEMENTS

I wish to express my sincere gratitude to Dr. R. Sharan and Dr. R.N. Biswas, my supervisors, for their invaluable guidance, comments and criticism throughout the tenure of this work.

I owe my thanks to Mr. H.K. Kanodia, Mr. R.S. Tomar, Mr. V.K. Agrawal and all my friends for their timely help and kind cooperation.

Thanks are also due to Mr. S.N. Sikdar and to the staff of Store, Dept. of Electrical Engg., I.I.T.Kanpur for extending me full cooperation in getting the components available in time.

The excellent typing by Mr. K.N. Tewari and ink-drafting by Mr. Syed Quasim Husain are appreciated.

January, 1978 K.K. Khurana

CONTENTS

LIST OF FIGURES

NOMENCLATURE

I_o	Bias current flowing through the device
I	Total current flowing through the device
σ	relative dynamic conductance
V_{jth}	threshold junction voltage
η	ideality factor of the diode
R	series resistance of the diode
T	temperature in degree kelvin
TE	thermionic emission
TFE	thermionic field emission
FE	field emission
k	Boltzmann's constant ($k = 1.38 \times 10^{-23}$ joule per degree kelvin)
m	modulation index
ω	radian frequency
g	dynamic conductance
C	capacitance
f	frequency in Hz
I_s	saturation current constant
i	instantaneous current
K	gain of the buffer
H	transfer gain
α	inverse Q-factor
v	instantaneous voltage
ϕ	phase difference
τ	time constant of an RC filter

r_e dynamic resistance of the diode

V_T temperature equivalent voltage ($= \frac{kT}{q}$)

m, n integers.

CHAPTER 1

INTRODUCTION

Derivative techniques are employed in many fields of science and engineering. Under many experimental conditions it becomes necessary to obtain the slope, curvature or other higher derivatives of the plots of interest. This can be obtained by getting the plot experimentally and then numerically calculating the derivatives from it. However, it is well known that numerical differentiation is prone to error, particularly in case of an experimental data where any error in experimental measurement affects the derivative calculation adversely. Due to this reason, effort has been made in many fields of scientific measurement to arrange the experiment in such a way that the first and higher order derivatives can be directly obtained. If sufficient care is devoted to the design of the experiment, it is found that accuracy of the experimental results becomes better as compared to the one that can be obtained numerically.

As far as the field of semiconductor devices is concerned, firstly, Hall[1], using a circuit designed by Tiemann[2] has successfully applied the differentiation technique to the current voltage characteristics of tunnel diodes at low temperatures. For similar work at the Bell Telephone Laboratories, A.G. Chynoweth and R.A. Logan[3] felt

a need not only for displaying the first derivative as a function of bias voltage but also of the second derivative. With such systems, structure that is invisible to the eye in the current voltage curves and only slightly apparent in the first derivative curve is dramatically displayed.

Much information can be obtained about the phonon process, and hence about the band structure, in semiconductors by a careful analysis of structure in the current voltage characteristics of tunneling junctions. The differentiation technique was applied to semiconductor tunneling junctions of III→V compounds[1] in order to present more clearly the polaron and phonon processes occurring during tunneling at liquid helium temperatures. By displaying the second derivative as a function of bias, the further increase in resolving power and sensitivity over the first derivative approach yielded more accurate data on prominent phonon effect as well as revealing more conclusively fine structure due to multiphonon emission and Stark splitting of the energy bands[3].

The electron tunneling into superconductors provides a powerful method for determining the energy gap, density of electron states, and phonon spectra of superconductors[4]. There are two quantities of primary interest in such measurements, (1) the relative dynamic conductance, $\sigma = (\frac{dV}{dI})_n / (\frac{dV}{dI})_s$, which can be obtained from measurements of dV/dI, the dynamic resistance of tunnel junction, with

both members in the normal state (n) and again with one or both members in the superconducting states (s). The quantity σ is related to the density of electron states of superconductors..(11) It is also of interest to measure $d\sigma/dV$, since structure in this quantity as a function of junction bias voltage V reflects features of the phonon spectrum of the superconductor.

The dependence of conductance on voltage for metal-insulator-metal junctions is, roughly parabolic but the minimum conductance need not occur at V = 0. Small deviations from this parabolic conductance behaviour are due to interactions of the tunneling electrons with impurities in the oxide, the oxide itself, or the surface layers of the metal electrodes. These emission processes are studied by even conductance and its derivative[5]. This derivative, at low voltages, is a crude measure of the phonon density in the normal metal electrode. It was shown that self energy effects in the normal metal can be conveniently displayed by calculating the odd conductance. R.C. Jaklevic and J. Lambe[6] showed that the tunneling electrons interact with vibrational modes of impurity molecules trapped in the insulating oxide layer. The excitation of such a mode gives rise to an increase in conductance (dI/dV) and thus the frequency of the modes can be determined from the derivative technique.

These techniques have recently been successfully applied to an analysis of the I-V characteristics of GaAs injection lasers[7,8]. The first derivative has been shown to be useful, both in homojunction and in double heterostructure lasers, by measuring the parameters entering the I-V characteristic as well as for extracting lasing thershold and other features intimately related to the lasing process. In an ideal laser, the separation of the electron and hole quasi fermi-levels, and hence the junction voltage, becomes pinned at threshold as a result of the high rate of stimulated emission[9]. The I-V relation for $I > I_{th}$ becomes $V = I R + V_{jth}$, where V_{jth} is the junction voltage at threshold. The derivative dV/dI above threshold is therefore, a constant equal to the series resistance R. Consequently at the lasing threshold, the product $I\frac{dV}{dI}$ should decrease abruptly from $IR + \frac{\eta kT}{q}$ to IR and then continue to increase with current at a rate equal to R, thus allowing accurate determination of the lasing threshold using derivative technique.

Paoli[9,10] investigated the behaviour of the second derivative of I-V characteristic of stripe geometry(AlGa)As junction lasers and its relation to the variation of the first derivative with current. In the vicinity of the lasing threshold, a pronounced peak occurs in the second derivative signal as a result of the voltage saturation

induced by the stimulated emission. Above threshold, the second derivative assumes non-zero positive values for lasers with incomplete saturation, while complete saturation is characterized by a near-zero value for the derivative. The above threshold behaviour of the second derivative also reveals the presence of perturbations in the saturated state of an otherwise well-behaved laser.

Our interest, which has led to the design of the present system, is in the study of metal-semiconductor junctions, where it is particularly difficult to know the mechanism of current transport. In cases of thermionic emission (TE), thermionic field emission (TFE) and field emission (FE) the plots of ηT versus T as discussed by Saxena[11] have been shown in Figure 1. Curve 1 corresponds to $\eta = 1$, whereas curve 2 corresponds to a value of $\eta > 1$. In case of curve 3 there is a parallel shift as compared to curve 1. Curves 1,2,and 3 represent thermionic emission. The curves 4 and 5 represent thermionic field emission and field emission respectively. The measurement of the parameter η at various temperatures will decide the mechanism of current transport in Schottky barriers. This parameter is related to the second derivative whereas R, the series resistance is related to the first derivative of the I-V characteristic of the device. Thus the present system which is capable of providing the I-V plot

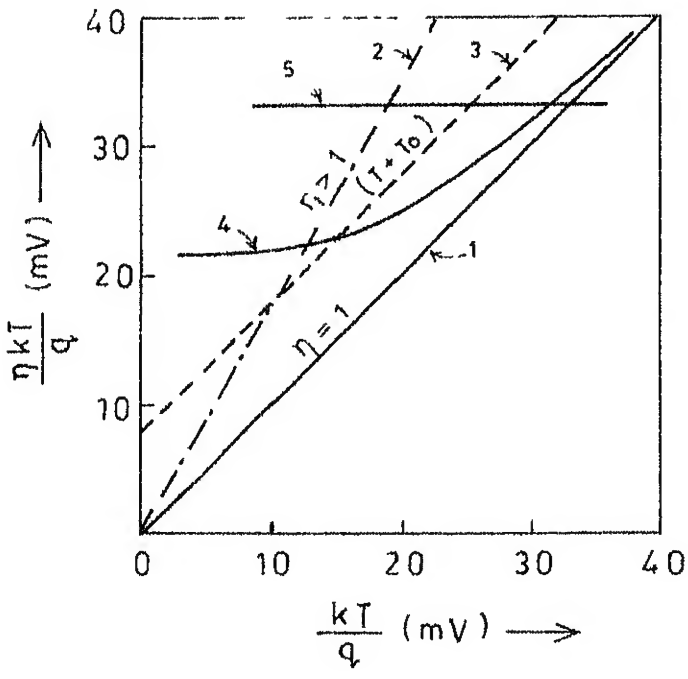

Fig. 1 Plot of $\frac{\eta kT}{q}$ versus $\frac{kT}{q}$ showing Thermionic, Thermionic Field emission and Field emission in schottky barriers.

as well as $I\frac{dV}{dI}$ and $I^2\frac{d^2V}{dI^2}$ versus I plots can be a good tool for the characterization of the metal-semiconductor junctions. Moreover, it will be a good scientific instrument for the research work related to the other derivative measurements.

In Chapter 2, the various techniques of derivative measurement have been discussed. A table has also been given with the remarkable features of each technique. In Chapter 3, the basic principle of the system is discussed. A brief description of various building blocks of the system is also presented. Chapter 4 deals with the circuit design of the system, whereas the next chapter brings out the meritorious features of it. In Chapter 6,a few semiconductor devices have been characterized and the results have been correlated.

CHAITER 2

REVIEW OF VARIOUS TECHNIQUES

2.1 Harmonic Detection[12]

2.1.1 Current Modulation:

The method employed to determine dV/dI and d^2V/dI^2 is to apply a small ac signal $i = I\cos\omega t$ superimposed on the dc bias voltage across the junction and then to detect the voltage at the fundamental and second harmonic frequency of this ac signal. If the current modulation amp. i is kept constant, then the voltage across the junction may be written in a Taylor series as:

$$V(I) = V(I_o) + \left(\frac{dV}{dI}\right)_{I_o} i\cos\omega t + \frac{1}{4}\left(\frac{d^2V}{dI^2}\right)_{I_o} i^2(1+\cos 2\omega t) + \ldots \quad (1)$$

Thus the component of the voltage at the fundamental frequency is proportional to $(dV/dI)_{I_o}$ and the component at the second harmonic 2ω is proportional to $(d^2V/dI^2)_{I_o}$. With a stable amplitude oscillator and a good lock-in amplifier, the method of harmonic detection can be applied directly to give measurement of dV/dI with an accuracy of 1 in 10^3.

If one is interested in obtaining a value of the conductance dI/dV from the measured resistance dV/dI, it is necessary to mathematically invert dV/dI. This can be done point by point or by use of a computer.

2.1.2 Voltage Modulation:

It is also possible to measure $(dI/dV)_{V_o}$ directly[4,13]. A constant voltage ac signal $v = V\cos\omega t$ is now applied to the junction superimposed on a voltage bias and the method of harmonic detection is employed to measure the current changes by measuring the voltage across a fixed value resistor. Very low modulation levels (5 to 10 μV rms) are employed in the circuit.

When the function of interest in derivative measurement is d^2I/dV^2, there are several methods by which this parameter can be obtained. A measurement of d^2V/dI^2 can be obtained by a number of methods[7,16] by monitoring the signal at the second harmonic rather than at the fundamental frequency. Having obtained a value for d^2V/dI^2 one can then use the identity $d^2I/dV^2 = (d^2V/dI^2)(dI/dV)^3$ to obtain a value for the derivative of the conductance.

2.1.3 Illustration:

A block diagram of the above system with the voltage modulation[14] is shown in Figure 2. The current measuring circuit, which has essentially zero input impedance, produces an output voltage proportional to the current in the device under test. The reference channel of the lock-in amplifier provides internal frequency doubling for d^2I/dV^2 measurements. The voltage across the sample is measured with a Keithley model 160 digital voltmeter, whose analog output

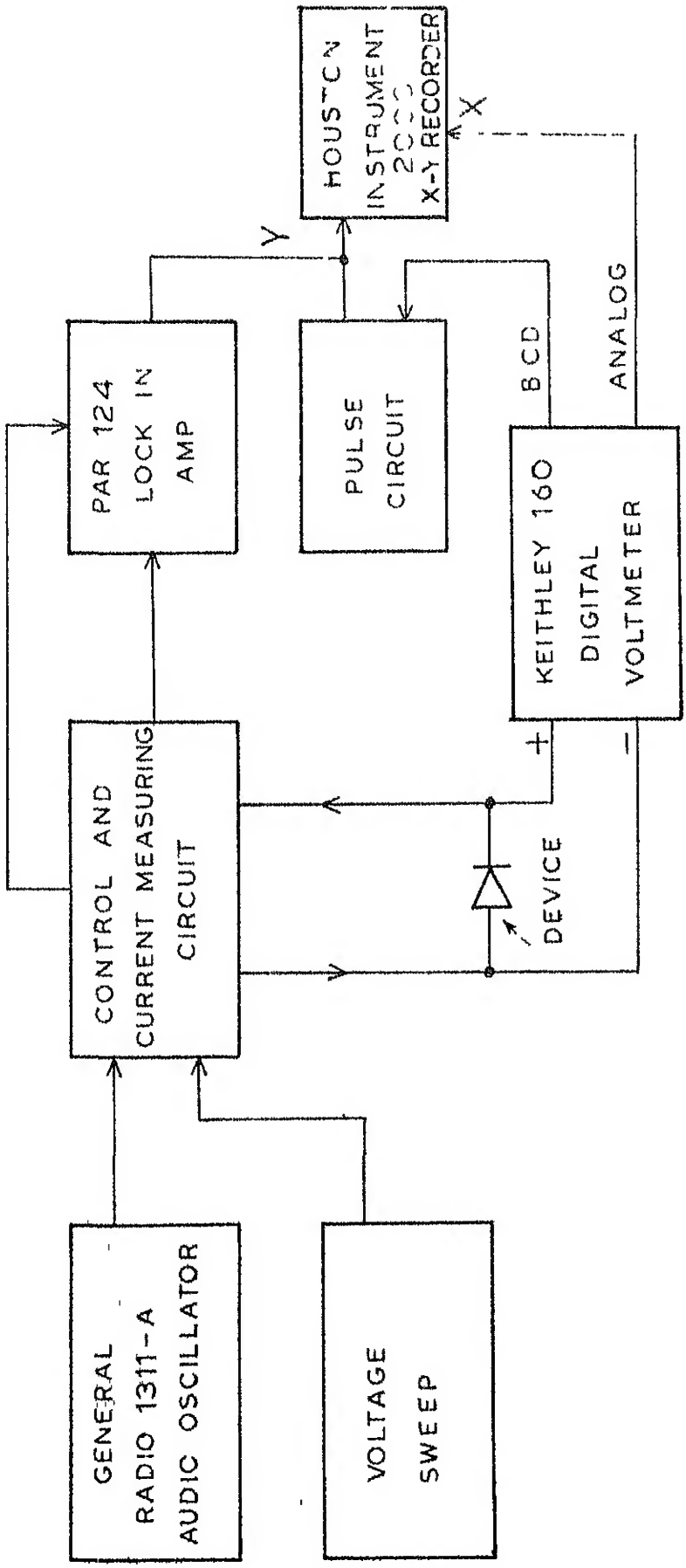

Fig. 2 Block diagram of the method developed by Korb and Holczyck

drives the X axis of the X-Y plotter. Because of the sensitivity of the current measuring circuit to small currents, including noise currents, it is essential that the high impedance (+) terminal of the DVM be connected to the low side of the sample. This polarity inversion is accounted for in the connection of the analog output of the DVM to the X axis of the recorder. In order that the mis-calibration of the X axis or expansion of the recorder sheets due to humidity does not lead to erroneous voltage ratings, the BCD output of the DVM is monitored and a simple pulse circuit produces a 1 cm blip of 0.1 sec.duration on the recorder sheet at desired intervals (usually 10 or 20 mV). A voltage sweep employs an integrator to produce a voltage ramp or dc bias for the junctions. A current amplifier provides bias current upto ± 3A.

2.2 Bridge Technique

Illustration:

This system[9] utilizes a bridge circuit and an opamp., the latter providing the inversion which is necessary in order to obtain conduction results from a resistance bridge.

If C_x and $g_x = dI/dV$ represent the capacitance and dynamic conductance of a junction in the Wheatstone bridge shown in Figure 3 and if $V_o\, e^{j\omega t}$ represents a constant sinusoidal voltage across the reference resistor R_s, opamp. will maintain the same across the junction. Two bridge

arm-currents labeled I will then be equal, and any conductance mismatch between the junction used and the reference elements R_s and C_s must be compensated by an additional current δ_1 from the amplifier.

The nonlinearity of I-V characteristic for the junction will also demand that the total current through the junction have a harmonic content if the voltage across it is to be a pure sinusoid. Since I is a pure sinusoid, δ_1 must contain these additional harmonics as well. One may get:

$$\delta v = V_o e^{j\omega t} + Z_f \delta_1$$

$$= \frac{1}{2} Z_f \{g_x - G_s + G_f + j\omega (C_x - C_s + C_f)\} V_o e^{j\omega t}$$

$$+ \frac{1}{4} Z_f g_x' V_o^2 e^{2j\omega t} + \ldots \qquad (2)$$

The circuit shown in Figure 3 therefore has the properties of a conductance bridge and variations in the dynamic conductance g_x may be followed with a phase sensitive detector. Since the signal across R_s will phase lag the oscillator signal, and since Z_f will cause an additional phase lag, the g_x part of the output signal δv will lag the oscillator signal by a constant phase angle. The correct phase setting for the reference channel of the phase sensitive detector may be found by first adjusting R_s and C_s to obtain $\delta v = 0$ as indicated by an oscilloscope and then increasing R_s by a small amount. The resulting signal then

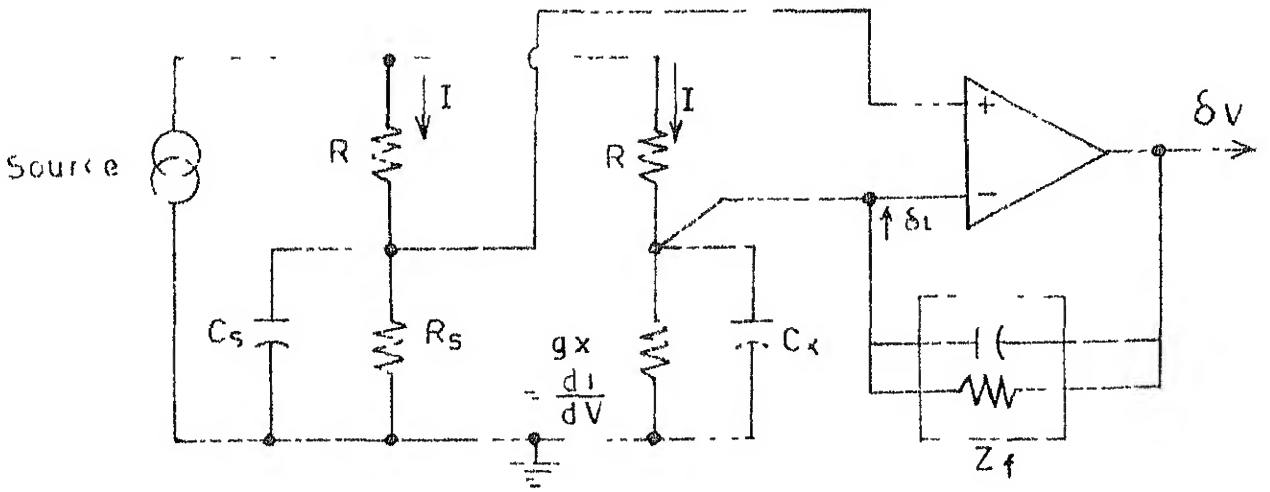

Fig 3 Conductance Bridge used by J S. Rogers.

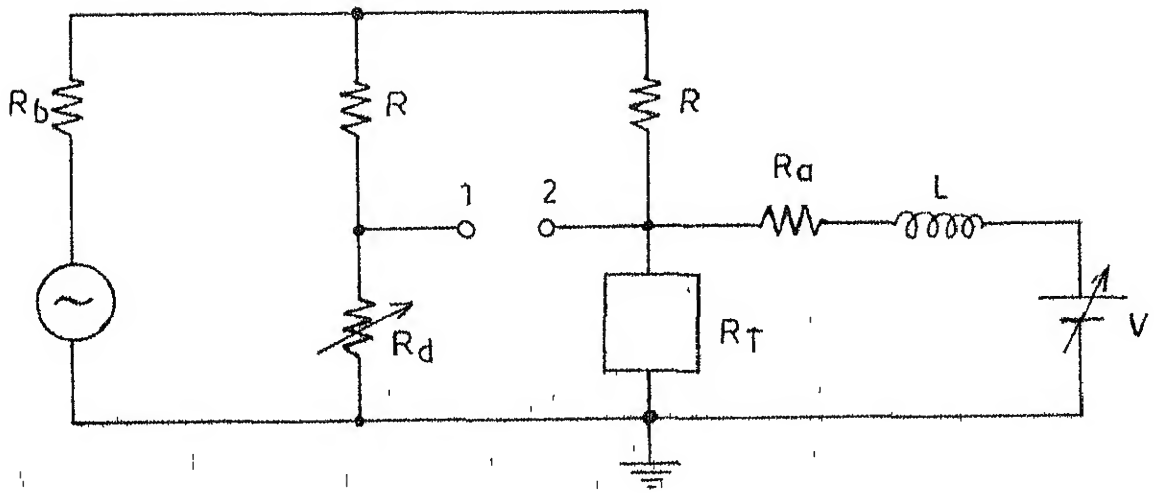

Fig. 4 Resistance Bridge used by Adler and Jackson

corresponds to an increase in g_x, and since it is free of quadrature components, the detector may be adjusted for maximum response to it. The same phase setting will then be correct for second harmonic detection as well if the oscillator frequency is accurately halved for second derivative recording.

2.3 Modified Techniques

2.3.1 Combined Harmonic Detection and Bridge Technique:

This system[4] uses a combination of harmonic detection and bridge techniques for the measurement of dV/dI and d^2V/dI^2.

The conventional harmonic detection methods using a preamplifier and a lock-in amplifier cannot provide the required high resolution. Since the junctions under consideration are only weakly nonlinear, the variation of interest comprises only a small part of the total signal across the junction so that most of lock in amplifier output signal (90 to 99%) must be bucked out in order to display these small variations on an X-Y plotter or similar recording device. Two difficulties immediately arise:

(i) the high gain required cannot always be attained because of the limited dynamic range of the lock-in amplifier, and

(ii) the significant errors may be introduced due to gain variations of the amplifier and instabilities in the bucking voltage.

These two difficulties may be overcome by bucking out most of the signal prior to amplification. Such a method has been applied by incorporating the junctions as one arm of an ac Wheatstone bridge. This method has an additional advantage in that it provides rejection of the fundamental ω, when measurements of d^2V/dI^2 are made. This cancellation of the fundamental is complete when the bridge is balanced, the signal proportional to d^2V/dI^2 is unaffected because the junction is the only nonlinear element of the bridge.

Previous use of an ac bridge required high modulation levels in the region of interest. Such modulation may produce serious smearing of the information.

The present bridge provides high resolution measurements of dV/dI and d^2V/dI^2 using low modulation levels. At these levels the resolution is limited by thermal rather than instrumental smearing at temperatures near $1^\circ K$.

As shown in Figure 4, one arm of the bridge contains semiconductor junction R_T, which is treated as a nonlinear passive element, while the other arm has R_d set so that $R_d \approx R_T$ and $R >> R_d$. The inductance L and the resistance R_a are large enough that one may neglect the ac shunting of the junction by the dc bias supply. Also R_b is large enough that shunting by the ac modulation supply can be neglected.

If $\delta \cos \omega t$ is the current in each arm then

$$V_1 = R_d \delta \cos \omega t$$

and
$$V_2 \approx I_o R_d + (dV/dI)_{I_o} \delta \cos \omega t + \frac{1}{4}(d^2V/dI^2)_{I_o} \delta^2(1 + \cos 2\omega t) + \ldots$$

Thus,

$$V_{12}(\omega) = \delta\{R_d - (dV/dI)_{I_o}\} \cos \omega t \qquad (3)$$

and
$$V_{12}(2\omega) = \frac{1}{4} \delta^2 (d^2V/dI^2)_{I_o} \cos 2\omega t \qquad (4)$$

Proper choice of R_d enables one to use the full scale of the recording device to display the small variation in dV/dI of the junction rather than dV/dI itself. In this way the problems of dynamic range and gain stability of the lock in amplifier are circumvented.

Adler et al[15] further developed an instrumentation for the measurement of the first and second derivatives and recording these on magnetic tape suitable for subsequent computer analysis. The system is capable of resolving changes in the first derivative as 1 in 10^5. The method of measurement employs a combination of harmonic detection and bridge techniques similar to that used above along with a data acquisition system which presents the data on digital magnetic tape.

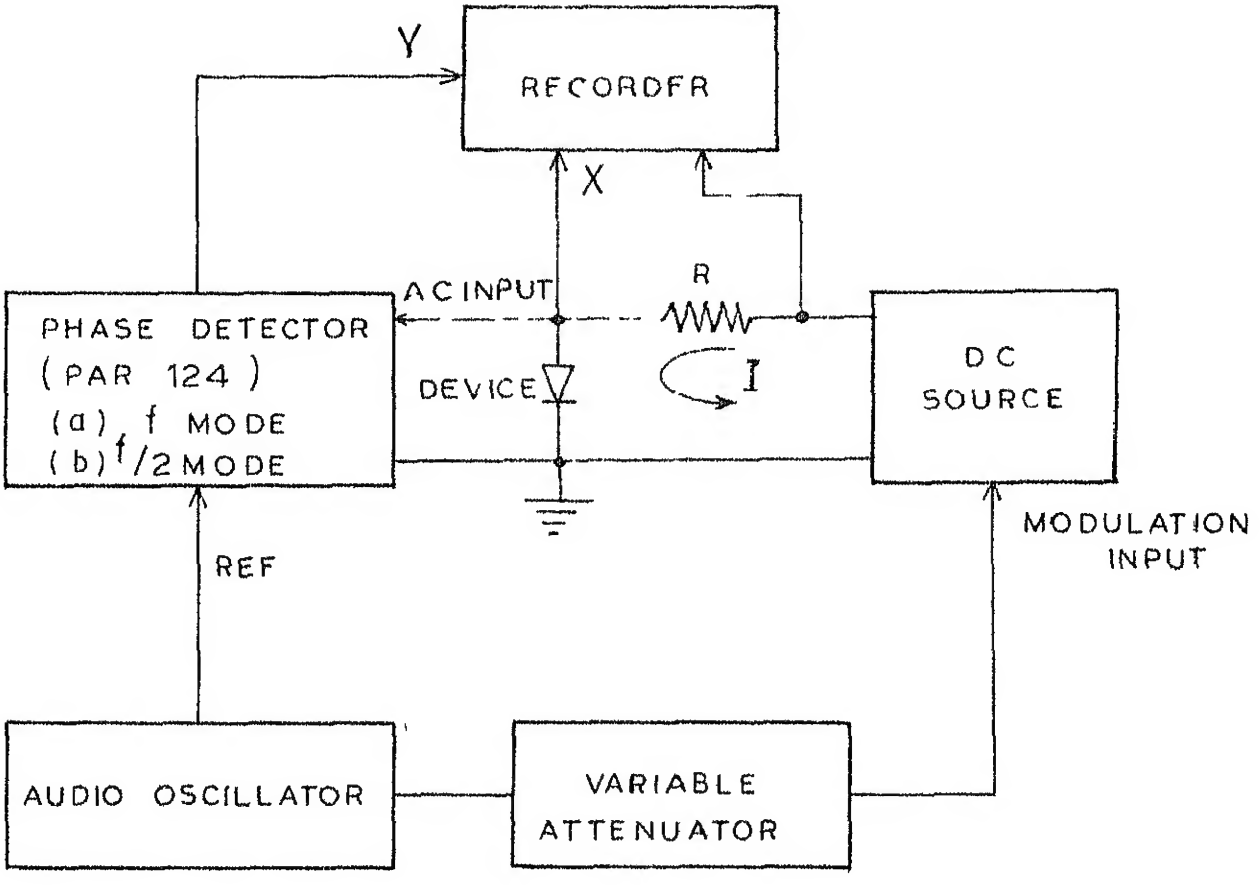

Fig 5 Block diagram for variable-depth current modulation technique.

2.3.2 Variable Depth Current Modulation Technique[7]:

As shown in Figure 5 the product $-I^2(d^2V/dI^2)$ has been obtained by detecting the second harmonic signal generated with a current modulation whose amplitude is increased in direct proportion to the increase in bias current I. With this type of modulation, the signals at ω and 2ω remain within the same order of magnitude over the entire range of currents, and detection of the second harmonic does not require a high rejection of the fundamental signal.

Detection at frequency 2f can be accomplished by operating the phase detector in the f/2 mode. In this mode, the instrument produces an internal reference frequency at exactly twice the frequency of the externally applied reference, thus making the detection system sensitive to V_{2f}.

2.3.3 Dual Frequency Constant Depth Current Modulation Technique[16]:

The principle and advantages of this technique are going to be discussed in Chapter 3. As shown in Figure 6(b) the current supplied to the diode is modulated at two phase-locked frequencies f_1 and nf_1. The coherent signals were derived from a signal generator (Hewlett Packard, Model 203A) with synchronous sinusoidal and square wave outputs at f_1. The distortion level (0.06% of this generator was more than adequate to

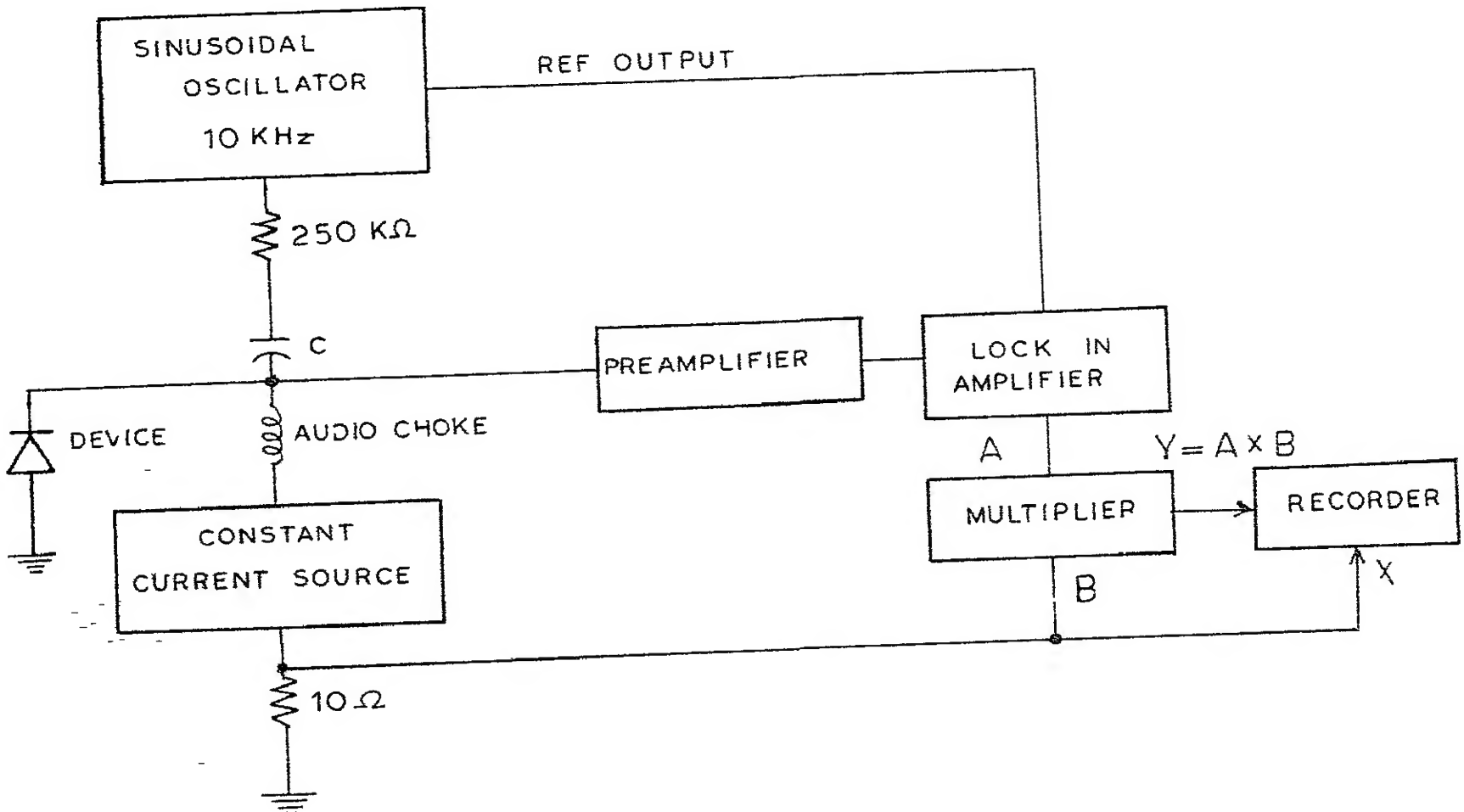

Fig. 6 (a) Block diagram for determinig the first derivative using Dual – Frequency Technique

elimination spurious contributions to the second derivative signal. The sinusoidal output was applied directly to the diode, while a coherent signal at nf_1 was derived from the square wave output by down converting its frequency to $(1 - n)f_1$ and then extracting the $\left(\frac{n}{1-n}\right)$th harmonic of the resulting squarewave to synchronize a phase locked oscillator. In the detection circuit, after passing through a low pass filter and amplified, the second derivative signal at $(1- n)f_1$ was detected with a lock-in amplifier (PAR Model HR8) Reference for the phase sensitive detection was obtained directly from the IC count-down circuit.

A few standard methods with their main features and some limitations have been presented in a tabular form on the next page.

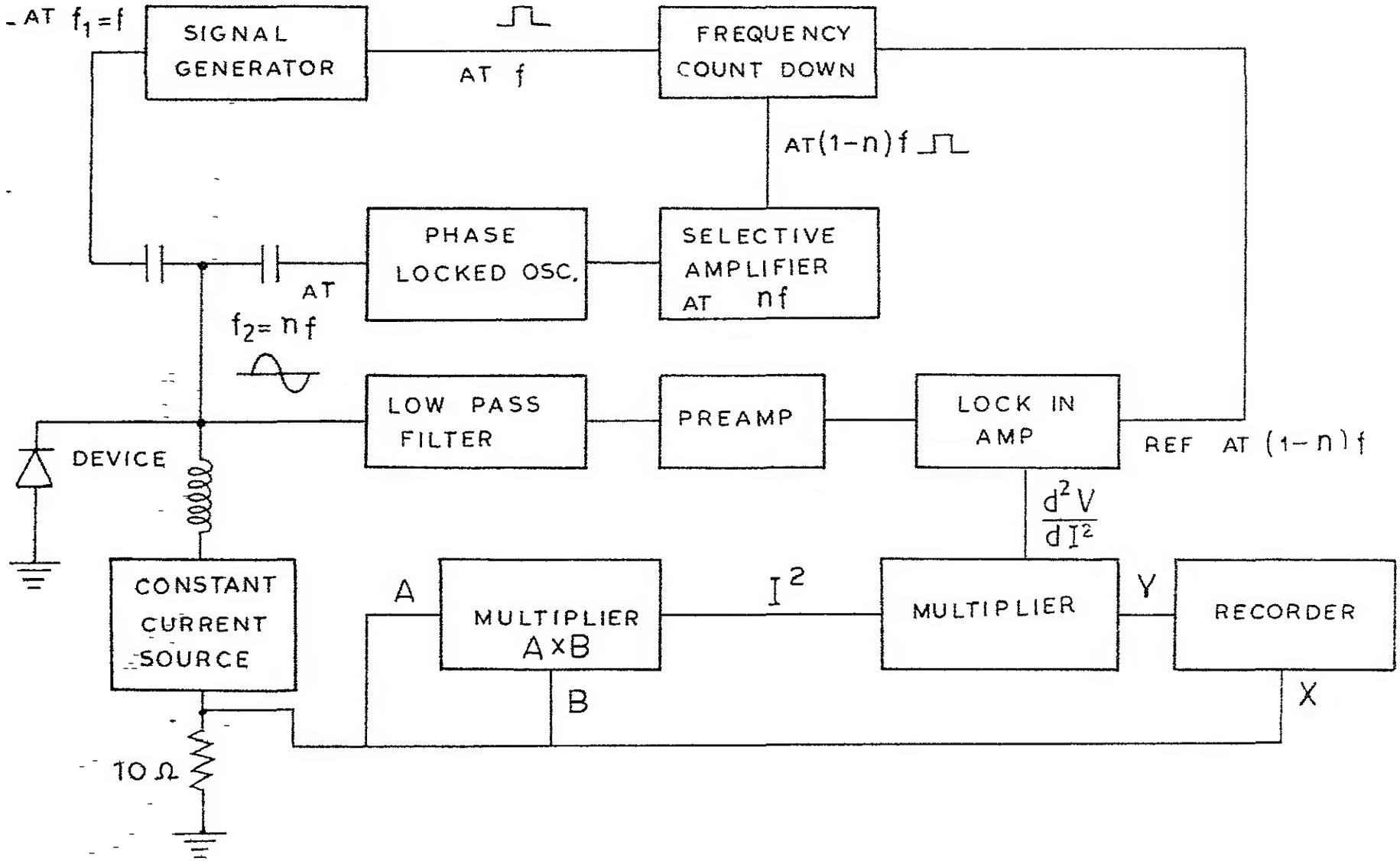

Fig. 6 (b) Block diagram for determining the second derivative using dual frequency technique

Table 1: Various Techniques of Derivative Measurement

S. No.	Developed by	Method used	Type of Modulation	Remarkable feature	Limitation
1	J.J. Tieman[2] (Oct.1961)	Harmonic detection	Voltage modulation	First effort for derivative measurement. Use of vacuum tubes. Wide impedance range.	Bulky, accuracy < 1 in 10^3
2	D.E.Thomas,[17] J.M.Klein (Aug. 1963)	Bridge technique	Voltage modulation	Use of servomechanism for detection	Costly, accuracy < 1 in 10^3
3	W.R.Patterson, J.Shewehun[18] (Dec. 1964)	Harmonic detection	Current modulation	Use of ring modulator for synchronous detection	Accuracy <1 in 10^3
4	J.G.Adler and J.E.Jackson[4] (Aug.1966)	Harmonic detection and bridge technique	Current modulation	High resolution measurements (1 in 10^5) with modulation levels below 60 μV rms	-
5.	W.R.Patterson, M.Kuhn[19] (July,1969)	Harmonic detection	Voltage modulation	Use of Lock-in amplifier for voltage detection. Extremely flexible in the range of sample impedances it will accept.	Accuracy-0.5%, Costly.
6	J.S.Rogers[13] (1970)	Bridge method	Voltage modulation	Sufficiently sensitive and accurate.	-

(continued)

(Table 1 continued)

S. No.	Developed by	Method used	Type of modulation	Remarkable feature	Limitation
7	H.W.Korb and N.Holonyak[14] (Jan.1972)	Harmonic detection	Voltage modulation	Suitable for devices with large impedance range (1 to 10^5 ohms). Versatile enough to find other laboratory uses.	Costly.
8	R.W.Dixon[7] (Sep.1976)	Harmonic detection	Variable depth current modulation	Use of lock-in amplifier and ac controlled dc current source	Costly
9	T.L.Paoli and Joseph F.Svacek[16] (Sep.1976)	Harmonic detection	Dual frequency current modulation	Use of lock-in amplifier, selective amplifier, phase locked oscillator and preamplifier. One of the best methods.	Costly.

CHAPTER 3

BASIC PRINCIPLE AND BLOCK-DIAGRAM OF THE SYSTEM

3.1 Theoretical Aspects

The technique used to measure the first derivative is similar to the well known analog derivative techniques. The procedure relies upon superimposing an ac modulation, $i\cos(\omega t)$ onto the dc bias current I applied to the device. As is well known the ac response of a nonlinear device to a weak modulation is best discussed in terms of a power series expansion in terms of the modulated parameter. If the current modulation amplitude i is kept small (relative to I) and constant, then the voltage v developed across the device terminals may be written as a Taylor power series expansion in the modulation signal,

$$v = V\{I + i\cos(\omega t)\}$$

$$= V_o(I) + i\cos(\omega t)\frac{dV}{dI} + \frac{i^2\cos^2(\omega t)}{2}\frac{d^2V}{dI^2} + \ldots$$

$$= \{V_o(I) + \frac{i^2}{4}\frac{d^2V}{dI^2} + \ldots\} + \cos(\omega t)\{i\frac{dV}{dI} + \frac{i^3}{8}\frac{d^3V}{dI^3} + \frac{i^5}{192}\frac{d^5V}{dI^5} + \ldots\}$$

$$+ \cos(2\omega t)\{\frac{i^2}{4}\frac{d^2V}{dI^2} + \frac{i^4}{48}\frac{d^4V}{dI^4} + \frac{i^6}{1536}\frac{d^6V}{dI^6} + \ldots\} \quad (5)$$

Let the two terminal device be modeled by an ideal p-n junction in series with a resistance R. Let it be characterized by a current I which varies exponentially with applied voltage V as

$$I = I_s \{ \exp \frac{(V-IR)}{\eta V_T} - 1 \} \qquad (6)$$

where I_s is the saturation current and η is an exponential parameter usually depends on the characteristic of the mechanism by which the current flows.

On substituting equation (6), one can get

$$v = V_{dc} + \cos(\omega t)\{ IR + \eta V_T \frac{2}{m}(1-\sqrt{1-m^2}) \}$$
$$- \cos(2\omega t)\{\eta V_T \frac{2}{m^2}(1 - \frac{m^2}{2} - \sqrt{1-m^2}) \} + \ldots \qquad (7)$$

If $m << 1$, only the leading terms of each frequency component need be retained, and thus

$$v = V_{dc} + i\frac{dV}{dI}\cos(\omega t) + \frac{i^2}{4}\cdot\frac{d^2V}{dI^2}\cos(2\omega t) + \ldots \qquad (8)$$

and also

$$v = V_{dc} + (R + \frac{\eta V_T}{I+I_s})i\cos(\omega t) - \eta V_T \frac{i^2}{4(I+I_s)^2}\cos(2\omega t) + \ldots \qquad (9)$$

For modulation levels m less than 10%, the errors, in the above approximation are less than 0.25% for the first derivative $\cos(\omega t)$ and less than 0.5% for the second derivative $\cos(2\omega t)$.

Thus the voltage detection at the fundamental frequency yields a direct indication of $\frac{dV}{dI}$ and thereby the values of R and ηV_T. Similarly, the signal at 2ω can be used to measure the second derivative d^2V/dI^2 directly.

Since I_s is many orders of magnitude less than the currents of interest, the equations (8) and (9) can be rewritten as

$$I(dV/dI) = R(I) + \eta V_T \qquad (10)$$

and $$I^2(d^2V/dI^2) = -\eta V_T \qquad (11)$$

provided that the parameters η, I_s and R are not functions of current.

In order to correlate the last two equations, one can write the identity:

$$-I^2(d^2V/dI^2) = I\frac{dV}{dI} - I\frac{d}{dI}\left(I\frac{dV}{dI}\right) \qquad (12)$$

Since $\frac{d}{dI}(I\frac{dV}{dI})$ is the slope of the I(dV/dI) curve at I, above equation shows that in general $-I^2(d^2V/dI^2)$ is the intercept at I = 0 of the tangent to the I(dV/dI) curve. In principle then, no information is obtained from the direct observation of $-I^2(d^2V/dI^2)$ that could not have been found from the variation of I(dV/dI) with current. Nevertheless, the direct observation of the second derivative can be extremely useful since it avoids the graphical extraction of data which can be very inaccurate in regions where the function I(dV/dI) is rapidly changing.

It is worth emphasizing that direct measurements of the quantities $I(dV/dI)$ and $-I^2(d^2V/dI^2)$ are desired as opposed to the synthesis of these quantities from other measured parameters. This improves both the measurement accuracy and the experimental simplicity.

The conventional techniques commonly involve sinusoidally modulating an independent variable, such as current or voltage, and detecting the ac response of the dependent variable. A measure of the first derivative of the electrical characteristic is then provided by the ac component of the device response at the frequency of modulation, while the second derivative is in principle proportional to the sinusoidal response at twice the modulation frequency.

In a practical realization of the second derivative measurement two problems are encountered[14]:

(i) Firstly, the detection of the second harmonic signal requires rejection of the fundamental signal, which for weakly non-linear characteristics can be one or more orders of magnitude greater than the harmonic signal. Adequate attenuation of the fundamental without appreciable loss for the second harmonic requires a frequency selectivity which is not easily attained. If adequate attenuation of the fundamental is not achieved, then the input preamplifier of the lock-in amplifier will saturate at gain setting less

than that required to detect the harmonic signal.

(ii) Secondly, any second harmonic component in the modulation signal, from whatever source, will produce a second harmonic voltage proportional to dV/dI rather than d^2V/dI^2, giving rise to a distorted d^2V/dI^2 plots.

3.2 Dual Frequency Technique

This technique, which is very much similar to the well known intermodulation method of distortion measurement, utilizes ac modulation at two distinct but synchronous frequencies f_1 and f_2 to produce a derivative signal at a difference frequency f, which is unique to the order of the derivative being measured. By appropriate selection of the frequencies, the frequency selectivity required is greatly reduced compared to that needed for conventional harmonic detection and may easily be attained by simple passive filters. In addition, the effect of spurious signals from harmonic distortion of the modulation signal is eliminated since the frequency f at which the desired derivative signal appears is not coincident with a harmonic of the modulating frequencies.

Again going back to equation (5) and substituting $v = V\{I + i_1 \cos(\omega_1 t) + i_2 \cos(\omega_2 t)\}$ and neglecting the small terms, one may get

$$v = \{V_o(I) + \frac{d^2V}{dI^2}(\frac{i_1^2}{4} + \frac{i_2^2}{4})\} + \frac{dV}{dI}\{ i_1\cos(\omega_1 t)+i_2\cos(\omega_2 t)\}$$

$$+ \frac{d^2V}{dI^2}\{\frac{i_1^2}{4}\cos(2\omega_1 t) + \frac{i_2^2}{4}\cos(2\omega_2 t) + \frac{i_1 i_2}{2}\cos(\omega_1+\omega_2)t$$

$$+ \frac{i_1 i_2}{2}\cos(\omega_1 - \omega_2)t\} \qquad (13)$$

In response to a current modulation applied at two frequencies f_1 and f_2, the linear term in the expansion gives rise to sinusoidal components of f_1 and f_2, each of which is proportional to the first derivative dV/dI. Analogously, the quadratic term in the series produces signals at $2f_1$, $2f_2$, f_1+f_2, and f_1-f_2, all of which are proportional to the second derivative d^2V/dI^2. In principle, the second derivative can be measured by the signal at $2f_1$ or $2f_2$. However, detection at the difference frequency $f = f_1-f_2$ can be advantageous for two reasons:

First, by appropriate selection of the frequencies, the frequency selectivity of conventional components can be used more effectively than with second harmonic detection. A conventional low pass filter tuned to the difference frequency can provide much more attenuation of the fundamental than a filter tuned to the second harmonic. In addition, the exact value of f can be selected for optimum S/N ratio in the detector for those cases which require maximum sensitivity.

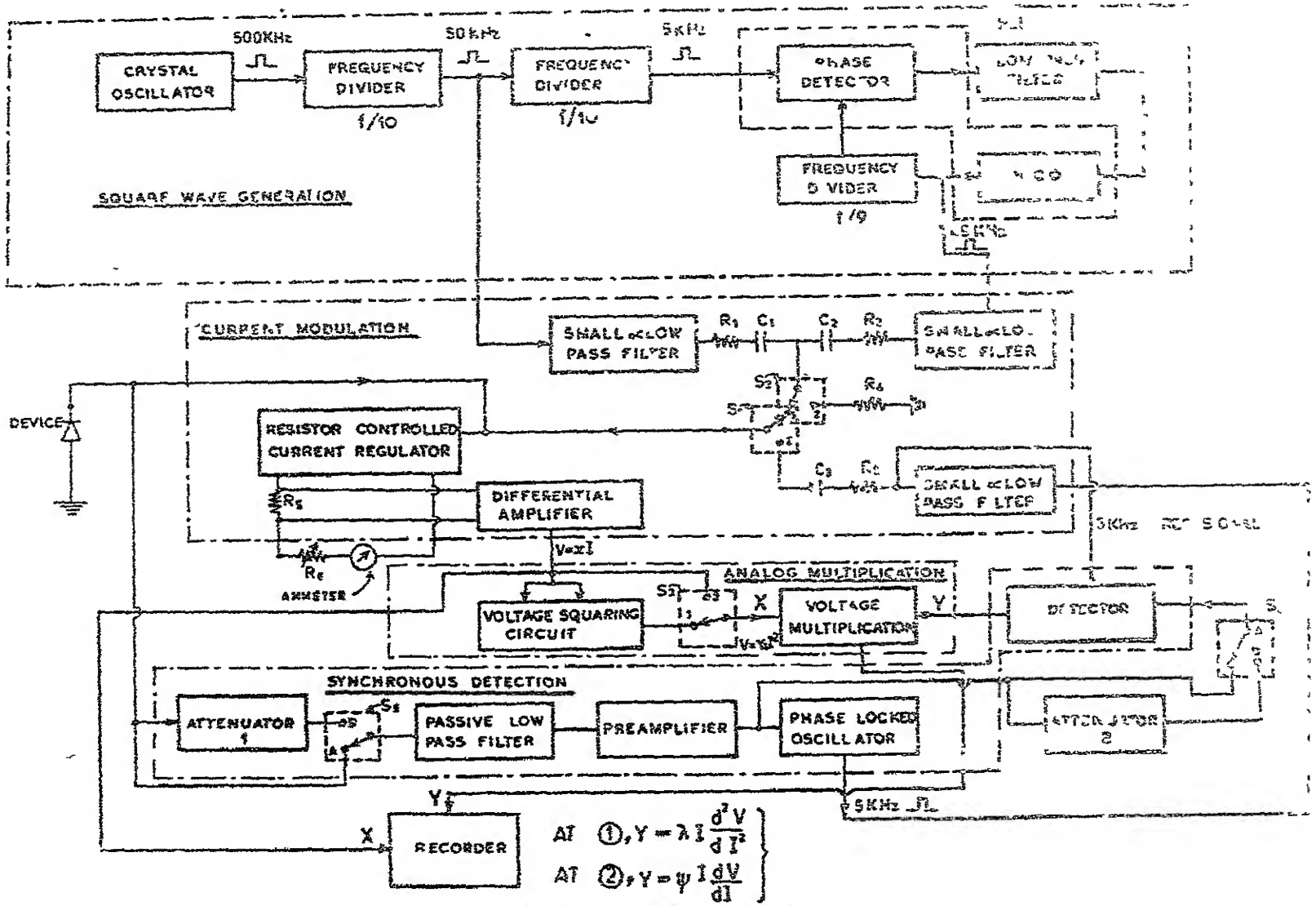

FIG.7 BLOCK DIAGRAM OF THE SYSTEM

Secondly, harmonic distortion of the modulation which produces a spurious signal proportional to the first derivative does not contribute to the second derivative measured at f_1-f_2. Consequently, the distortion requirements imposed on the modulator are less stringent with detection at the difference frequency than with second harmonic detection.

Dual frequency technique originally used by Paoli[16] is the heart of the present system which is going to be discussed blockwise in the next section.

3.3 Description of the system

As shown in Figure 7 the system may be divided into four parts based on function performed by them:

(i) Square wave generation

(ii) Current modulation

(iii) Synchronous detection

(iv) Analog multiplication

3.3.1 Square wave generation:

A standard crystal is used to generate 500 KHz square wave. Two digital counters have been used to divide the frequency to 50 KHz and 5 KHz respectively. A PLL with another counter of modulus 9 is used to generate 45 KHz square wave, from the 5 KHz square wave signal.

3.3.2 Current modulation:

Two small σ low pass filters have been used to filter out the odd harmonics. Thus after this stage we get two sinusoidal frequencies of 50 KHz and 45 KHz with high stability (being equal to the stability of the crystal) and distortion level less than 0.1%. These sinusoidal frequencies of 45 KHz and 50 KHz are used as modulating frequencies.

The two terminal device is biased with a constant current source, the current of which can be increased upto 300 mA by a variable resistor R_6 controlled from outside. The same current I also flows through the resistor R_5, the voltage across which is sensed by a differential amplifier to give a voltage directly proportional to the corresponding current.

Switches S_1 and S_2 when switched to positions (1) present two modulating frequencies 50 KHz and 45 KHz to the biased device, whereas in position (2), only a single frequency of 5 KHz is applied. Resistors R_1 and R_2 are sufficiently high to ensure that the modulation at these frequencies are with constant ac currents and secondly that $i \ll I$. In order to get good resolution, the permissible excursion of the ac signal about the dc bias point is kept very small as compared to the thermal energy KT = 25.8 meV at room temperature in order that the resolution be limited by thermal rather than instrumental smearing. The capacitors C_1 and C_2 are sufficiently high so that they may offer reactances of only

a few ohms but block dc coming from current regulator. Resistor R_4 is of a few tens of ohms and its purpose is to provide a low resistance path to the currents coming from the two ac sources and hence to avoid their interference when switch is at position 2.

3.3.3 Synchronous detection:

With switch S_1 and S_2 in position (1) from the modulated waveform, the strong fundamental signals at 45 KHz and 50 KHz are rejected with an RC passive filter to sufficient attenuation. Here the passive nature[20] of the filter is preferable because (i) they are least sensitive and hence best fit for handling the small signals, (ii) if it be active filter it would have its output saturated by strong fundamentals.

With switch S_1 and S_2 in position (2), there is only one modulating signal of 5 KHz which will directly pass through the low pass filter with a small percentage of second harmonic. It is quite possible that due to the larger fundamental signal (here at 5 KHz) the preamplifier may be saturated. Attenuator (1) is here to avoid this condition.

Thus after filtering and preamplification, the signal of 5 KHz frequency is passed to a synchronous detector. To the other input of the detector another 5 KHz signal phase locked to the first one is applied.

The output when properly filtered out gives the dc voltage which is the measure of d^2V/dI^2 with switches at position(1) and dV/dI with switches at position (2).

3.3.4 Analog multiplication:

The voltage V = xI is fed to a voltage squaring circuit which is actually a voltage multiplier with the two inputs connected to V = xI, thus getting $V^2 = x_1 I^2$, where x, x_1 are constants.

As shown, the next stage is a voltage multiplier. With S_1, S_2 and S_3 all at (1), the two inputs of the multiplier are $V = x_1 I^2$ and $V = y_1(d^2V/dI^2)$ and the output being equal to $V = \lambda I^2(d^2V/dI^2)$. The same voltages for all the three switches at (2) are V = xI, $V = y_2(dV/dI)$ and $V = \psi I(dV/dI)$ respectively.

The output of the voltage multiplier is applied to the Y input of the recorder, the X input of which varies linearly with bias current I.

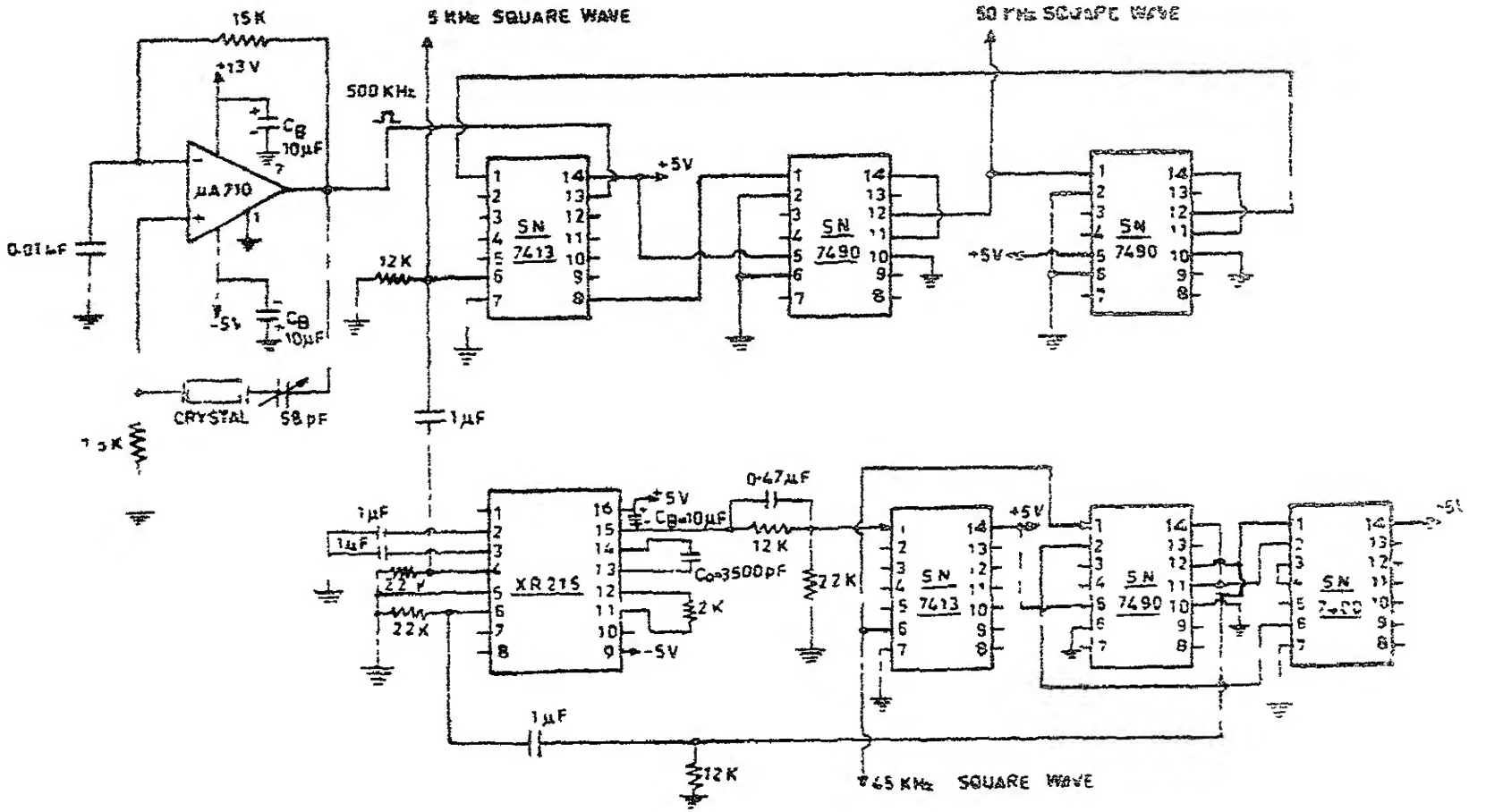

FIG.8 CIRCUIT DIAGRAM FOR SQUARE WAVE GENERATION

CHAPTER 4

CIRCUIT DESIGN

The system design has been presented in the same four parts as were discussed in the previous chapter.

4.1 Square Wave Generation

4.1.1 Crystal oscillator:

In the present technique, the difference-frequency signal should be of the same frequency and phase as that of the signal at the reference frequency. Thus, the frequency stability of the modulating signals must be better than 20 ppm/°C and hence signals must be derived from a crystal oscillator.

Commercial crystals are readily available at frequency greater than 100 KHz and this frequency will have to be divided to get the desired one. Due to the availability of digital circuits for frequency division it is preferable to generate the square wave signal rather than the sinusoidal one from the crystal used.

In order to facilitate the filtering of the difference frequency signal from those of the two modulating signals, let the latter be 9 to 10 times the former one. The modulating signals at 50 KHz and 45 KHz and hence the difference frequency signal at 5 KHz is sufficiently good approach.

A large number of circuits are available for generating square wave signal using a crystal , and

a JFET, a Schmitt trigger, a comparator etc. In our system, a comparator μA 710 has been used. It has fast response time (less than 40 ns) and moreover it is digitally compatible. It needs two unsymmetric supply voltages as shown, but since the same voltages are needed elsewhere, it is not a disadvantage.

The circuit used is similar to a free running multivibrator circuit, except that the positive feedback is obtained through a quartz crystal. The circuit oscillates when transmission through crystal is at a maximum, so the crystal operates in its series resonant mode. In our system the value of the capacitance used in series with the crystal is adjusted to a value of about 68 pf to generate square wave of exactly 500.000 KHz. The series capacitance used as well as the presence of very high input impedance of the comparator minimizes loading of the crystal and contributes to the frequency stability. The dc stability, which insures starting, is provided by negative feedback through a 15 K Ω resistor. The negative feedback is reduced at high frequencies by a 0.01 μf capacitor. A better square wave symmetry can be achieved by adjusting the dc voltage at the non-inverting input of the comparator. In the present case the generated waveform is to be divided by 10, through a decade counter which will automatically generate a symmetric square wave signal, hence the waveform symmetry is of no worth to be considered at this stage.

4.1.2 Frequency divider:

The decade counter SN 7490 has been used for frequency division. It has been used to divide the 500 KHz square wave signal to get 50 KHz square wave signal, which is again divided by 10 using another counter to get a square waveform of 5 KHz frequency.

4.1.3 Frequency multiplier:

By inserting a frequency divider into the feedback loop, between the VCO output and the phase comparator input, a PLL system can function as a frequency multiplier. The counter divides down the VCO frequency by the modulus, N. Thus when the entire system is phase locked to an input signal at frequency, f_s, the VCO output is at frequency Nf_s. By proper choice of the divider modulus, a large number of discrete frequencies can be synthesized from a given reference frequency.

The same principle has been employed to generate 45 KHz square wave, with a 5 Khz square wave as the input signal. PLL used is XR215[27] which can be operated over a large range of power supply voltages (from 5 V to 26 V), has a wide frequency band (0.5 Hz to 35 MHz), and is digitally compatible. Moreover its VCO has adequate frequency stability (typically 250 ppm/°C) and possesses lower rise and fall time (20 ns).

The design procedure may be summarized as follows:

(a) Without additional ICs, counter SN7490 can provide frequency division by two, five and ten. For getting frequency division by nine, the state 1001 need be decoded and fed to the $R_0(1)$ or $R_0(2)$ pin with $R_9(1)$ or $R_9(2)$ grounded. Since both the most significant bit (D) and the least significant bit (A) are 1 only in the last state, it is sufficient to generate AD, which has been obtained using two gates of the quad NAND logic SN7400.

(b) It is preferable here to have VCO frequency nearly equal to 45 KHz. The free running frequency f_o is approximately given by:

$$f_o = \frac{200}{C_o}\left(1 + \frac{0.6}{R_x}\right) \qquad (14)$$

where C_o is in μf, and R_x, the frequency range extension resistor is in KΩ. Here, f_o(= 45 KHz) is not sufficiently high, hence R_x can be open circuited. From expression (14) approximate value of C_o is 4444 pf. However practically the value needed is 3500 pf and has been used.

(c) The low pass filter capacitor is normally chosen to provide a cut-off frequency equal to 0.1% to 2% of the signal frequency, f_s. The internal impedance for the low pass section is 6 KΩ and thus two capacitors each of value 1 μf at the input terminals will serve the purpose.

(d) The lock range $\Delta\omega_L$ is given by

$$\Delta\omega_L = K_d K_o$$

where K_o (VCO conversion gain)

$$\approx \frac{700}{C_o R_o} \text{(radians/sec)/volt} \qquad (15)$$

(C_o and R_o are in μf and KΩ respectively)

and K_d (phase comparator gain)

≈ 2V/rad. (for signal amplitude greater than 100 mV).

Thus

$$\Delta\omega_L = \frac{1400}{C_o R_o} \text{ cycles/sec.} \qquad (16)$$

The capture range $\Delta\omega_C$ is given by

$$\Delta\omega_C = (\Delta\omega_L/\tau_1)^{\frac{1}{2}}$$

where τ_1 is filter time constant.

If R_o is chosen to be equal to 2 KΩ, the lock and capture ranges are approximately 400 Kdz and 8 KHz respectively, and ensure stability of the system.

(e) The phase comparator inputs should be at the same dc level with the bias current nominally 8 μA. Two resistors each of 2.2 KΩ connecting these pins to ground serve this purpose.

(f) The VCO produces approximately 2.5 V_{pp} output signal. The dc output level is approximately 2V below V_{cc}. This signal as such cannot be directly connected to a digital IC.

As shown the dc level is reduced down by a potential divider arrangement using two resistors of 2.2 K Ωand 12 KΩ, the output of the VCO being ac coupled to the counter.

4.2 Current Modulation

4.2.1 Active low pass filters:

The filter circuits to be preferred for our system should have the sensitivity as low as possible to the variation of the circuit parameters. The high slew rate opamps need frequency compensation,which is usually difficult for the closed loop gains not being an integral ratio. Hence, the commercial buffers,which are internally frequency compensated are preferable for our purpose.

The active filters discussed by Rao, Venkateswaran[25]; and Soderstrand, Mitra[26], as shown in Figure 9 are thus most suitable for our purpose. In analysing such circuits the most important parameter which was neglected by them is the departure of the gain of the buffer from unity particularly at high frequencies. The exact analysis, taking this inadequacy into account, is presented in Appendix 3. The resulting expressions relevant for the design are as follows.

The transfer function is given by

$$H(s) = \frac{V_o}{V_1} = \frac{1}{S^2 \frac{C_1C_2R_1R_2}{K^2} + S\{\frac{C_2R_2}{K^2} + (\frac{1}{K^2} - 1)C_1R_1\} + \frac{1}{K^2}}$$

$$= \frac{K^2/C_1C_2R_1R_2}{S^2+S(\frac{1}{C_1R_1} + (1-K^2)\frac{1}{C_2R_2}) + \frac{1}{C_1C_2R_1R_2}} \qquad (17)$$

where, the gain of the two buffers are assumed to be the same and equal to K.

Comparing the above equation to the standard form for the low pass filter:

$$H(s) = \frac{H_o \omega_o^2}{S^2 + \alpha\omega_o s + \omega_o^2} \qquad (18)$$

we have,

$$f_o = \text{centre frequency} = \frac{1}{2\pi (C_1 C_2 R_1 R_2)^{\frac{1}{2}}} \qquad (19)$$

$$\alpha = \frac{1}{Q} = (C_2R_2/C_1R_1)^{\frac{1}{2}} + (1-K^2).(C_1R_1/C_2R_2)^{\frac{1}{2}} \qquad (20)$$

$$H_o \text{ (the low frequency gain)} = K^2 \qquad (21)$$

and $$H|_{f=f_o} = K^2/\alpha \qquad (22)$$

Thus by minimizing α with respect to any of the parameters C_1, R_1, C_2, R_2 a low pass filter may be employed for the proper rejection of undesired frequencies.

From equation (20) the minimum value of α achievable is given by

$$\alpha_{min} = 2\sqrt{(1-K^2)} \qquad (23)$$

and thus,

$$C_2R_2/C_1R_1 = 1-K^2 \qquad (24)$$

For a square wave symmetrical about 0 V, Fourier series is given by

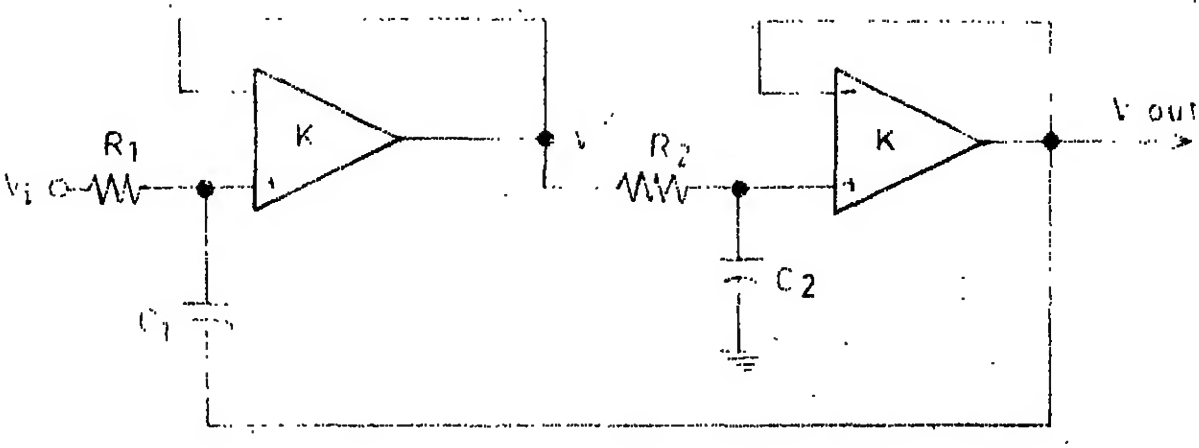

Fig.9 A low-sensitive Low-pass filter

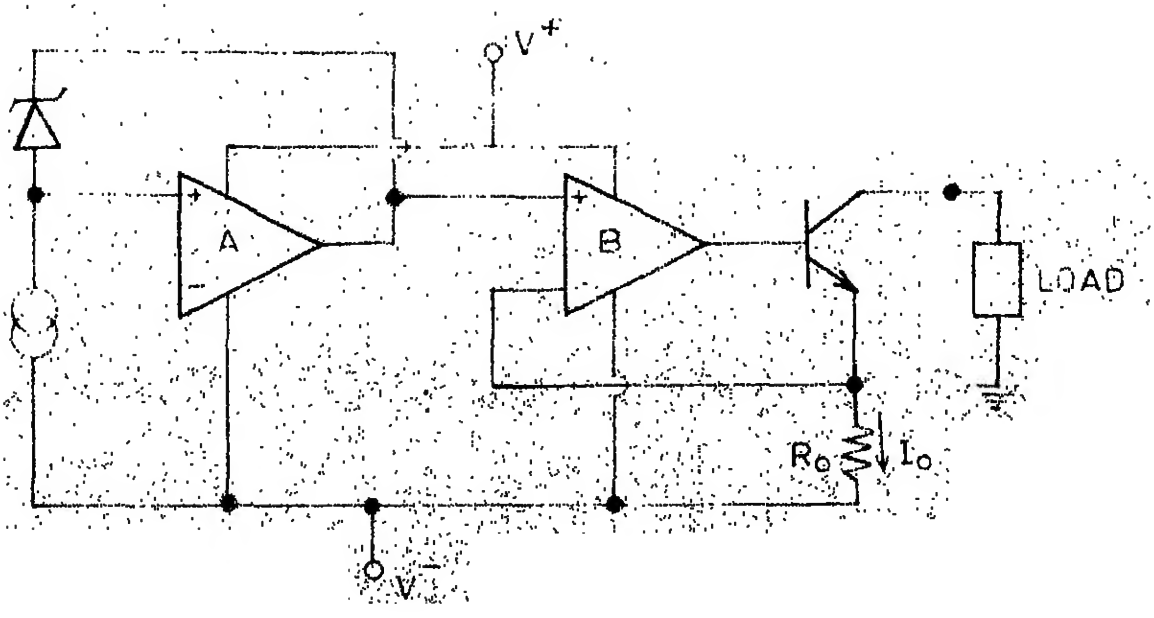

Fig.10 A Current regulator

$$v = \frac{V}{\pi} \left(\sin \omega t + \frac{1}{3} \sin 3 \omega t + \frac{1}{5} \sin 5 \omega t + \ldots \right) \tag{25}$$

Thus the content of third harmonic is one third of the fundamental and hence, in order to properly filter out the third harmonic content from the fundamental (say with a rejection ratio of 100), one should choose α_{min} in such a way that

$$\frac{V_o(f_o)}{V_o(3f_o)} = \frac{100}{3} \quad \simeq 30 \text{ db} \tag{26}$$

A glance over the amplitude versus frequency response of a second order low pass filter with α as the parameter necessitates $\alpha_{min} \leq 0.3$ for the above desired third harmonic rejection.

Design calculations:

Using IM310[28] as buffer, the minimum α obtainable at 50 KHz, 45 KHz and 5 KHz as calculated from equation (25) have been given below:

Frequency	Gain	α_{min}
50 KHz	0.992	0.26
45 KHz	0.993	0.16
5 KHz	0.999	0.06

Now using equations (19) and (24), the values of various components chosen are tabulated below (Choice, R_1 = 30 KΩ and C_1 = 1000 pf for 50 KHz and 45 KHz, C_1 = 0.01 μf for 5 KHz) :

f_o	R_1	R_2	C_1	C_2
50 KHz	30 KΩ	600 Ω	1000 pf	470 pf
45 KHz	30 KΩ	801 Ω	1000 pf	470 pf
5 KHz	30 KΩ	666 Ω	0.01 μf	4700 pf

Note: If suppose a filter is designed for $\alpha = 0.1$ with the assumption of buffers gain as unity, then for the actual value of K, $\alpha = 0.26$ at $f_o = 50$ KHz. Thus the error of 160% from the theoretical value ensures the importance of this parameter.

4.2.2 Current regulator:

As shown in Figure 9 the voltage at the non-inverting terminal of the opamp. B will be maintained at V_{ref}. The current coming out of the collector of the output transistor will be approximately the same as that through the resistor R_o. Thus the current through the load is given by $I_o = V_o/R_o = V_{ref}/R_o$

Any tendency of I_o to change will be reproduced by a change in V_o. This change is fed back to the input through the inverting terminal of the opamp resulting in a correction which restores both V_o and I_o to their original values. The output impedance of the current regulator discussed is equal to the collector to base impedance of the output transistor.

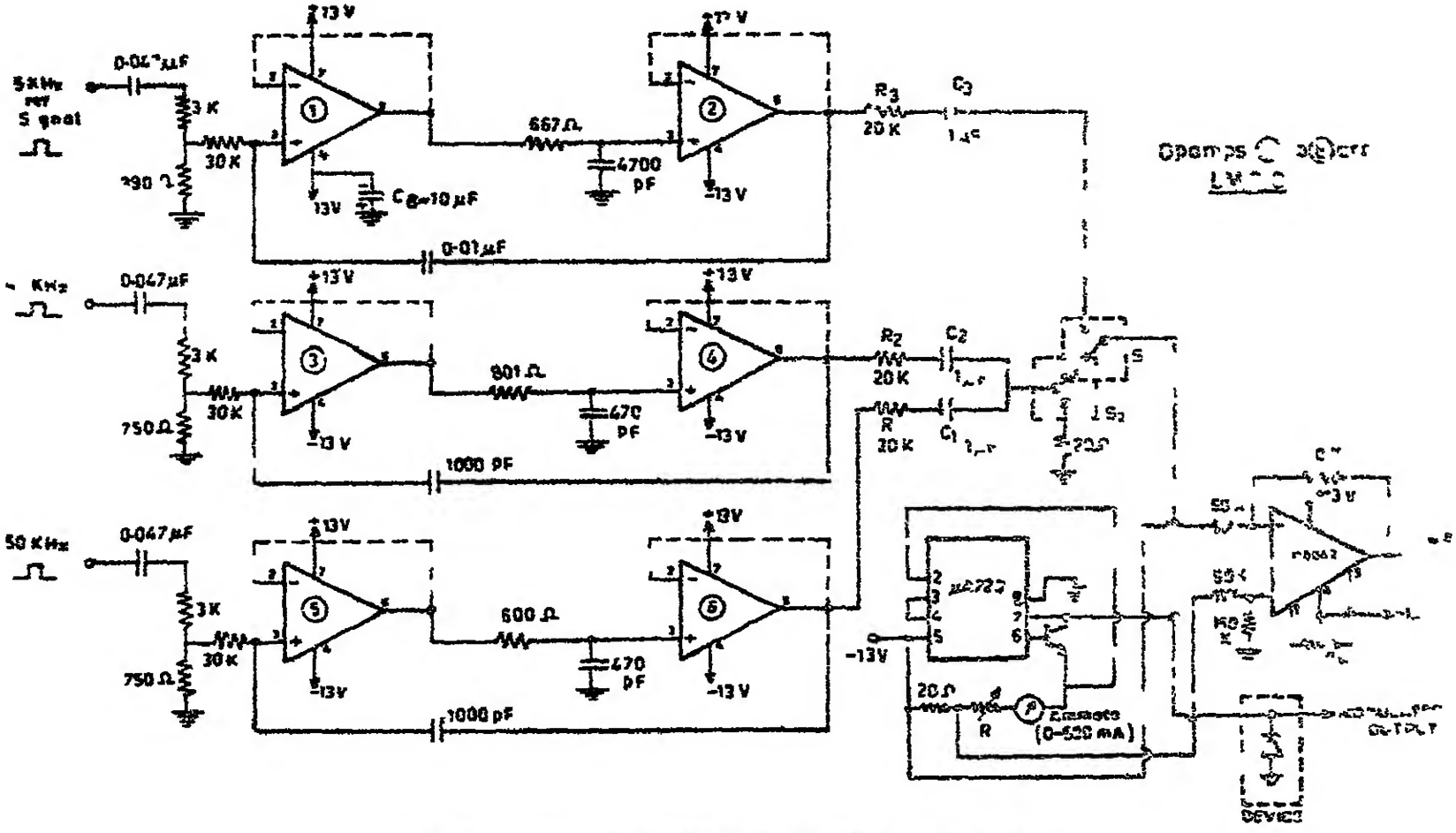

FIG 11 CIRCUIT DIAGRAM FOR CURRENT MODULATIC

All the constituent blocks needed for the synthesis of current regulator are there in IC μA723[28]. It consists of a temperature compensated reference amplifier, error amplifier, power series pass transistor and current limit circuitry. However, its output current is limited to 150mA. Our purpose is to make the system useful for devices ranging from solar cell, Schottky barrier to laser etc., hence output current upto 300 mA is achieved using additional npn pass element. Thus the arrangement shown gives an output current from 0 to 300 mA and has a provision to externally indicate its value. The small resistance of 20 ohms used serves two purposes: firstly it limits the maximum current and secondly the voltage across it is a measure of current flowing in the load.

4.2.3 Modulation:

The bias current I_o is passed through the device to be characterized. The 45 KHz and 50 KHz outputs have been connected through resistances (here 20 K-ohm) sufficiently higher than the dynamic resistance of the device for constant depth current modulation. Here these modulating currents are 0.12 mA(pp) so as to provide better resolution. Two large capacitors have also been connected in series with 20 K-ohm resistances so as to offer very small reactances at these frequencies and secondly for isolating the ac sources from the bias current. Since the output impedance of the

current regulator is of the order of M Ω, hence there is no need of any inductive reactance to isolate it from the ac sources.

4.2.4 Differential amplifier:

The voltage across 20 ohms resistor has been used to give a measure of the current flowing through it. The FET-input opamp LH0042 has very closely matched input characteristics, ultra low input currents (15 pA), very high input impedance (10^{12} ohm) and extremely high CMRR (86 db). This opamp has been used for providing the single ended output voltage proportional to the bias current.

4.3 Synchronous Detection

4.3.1 Passive low pass filter:

The order of the ac voltage sitting on the bias is just a few mV, hence a filter least sensitive to bias, temperature variation etc. will be preferred. Moreover, since in the dual frequency technique, the undesirable frequencies are very much apart from the desirable one, hence a simple passive filter will serve the purpose. For better filtering three RC sections have been used.

4.3.2 Preamplifier:

The signal obtained (of the order of a few mVs) after the low pass filter is too small to be useful for further processing. Therefore preamplification is essential.

The IM381 is a dual preamplifier specifically designed to meet the requirements of amplifying low level signals in low noise applications. Total equivalent input noise is typically 0.5 μV_{rms}. Other outstanding features include high gain (112 db), large output voltage swing $(V_{cc}-2V)_{pp}$, and wide power bandwidth (750 KHz, 20 V_{pp}) and being internally compensated and short circuit protected.

To achieve low-noise performance[30], special consideration must be taken in the design of the input stage. The input should be operated single ended, since both transistors contribute noise in a differential stage degrading input noise by the factor $\sqrt{2}$. Thus for optimum noise performance one input transistor is turned off and feedback is brought to the emitter of the first. The impedance of the feedback summing point is now two orders of magnitude lower than the base of the second transistor ($\simeq$ 10 KΩ). Therefore, to preserve bias stability, the impedance of the feedback network must be decreased. The feedback current is < 100 μA worst case. Therefore, for single ended input, resistors R_4 and R_5 are

$$R_5 = V_{BE}/5I_{FB} = 0.6/(5\times10^{-4}) = 1200\Omega \quad \text{(max.)} \tag{27}$$

$$R_4 = \left(\frac{V_{cc}}{1.2} - 1\right) R_5 \tag{28}$$

The design steps are as follows:

(a) Taking care of the restriction imposed R_5 has been taken to be 1 K-ohm.

$$R_4 = \left(\frac{V_{cc}}{1.2} - 1\right)R_5$$

$$= \left(\frac{26.0}{1.2} - 1\right)R_5$$

$$\simeq 20 \text{ K-ohm}$$

(b) The mid band gain is set by resistor ratios $(R_4+R_6)/R_6$. Let it be 1000, so that R_5 is approximately 20 ohm.

(c) Capacitor C_2 sets the low frequency 3 db corner where $XC_2 = R_6$. Thus

$$C_2 = \frac{1}{2\pi f_o R_6}$$

$$= \frac{1}{2\pi(800)(20)}$$

$$\simeq 10 \mu F$$

4.3.3 Phase locked oscillator:

Phase locked loop NE565[32], has been used to generate a 5 KHz square wave of the same phase as that of the difference frequency signal. The design formulas related to it are summarized below:

Free running frequency of VCO, $f_o = 1.2/4R_1C_1$ Hz (29)

Lock range $f_L = \pm 8f_o/V_{cc}$ Hz (30)

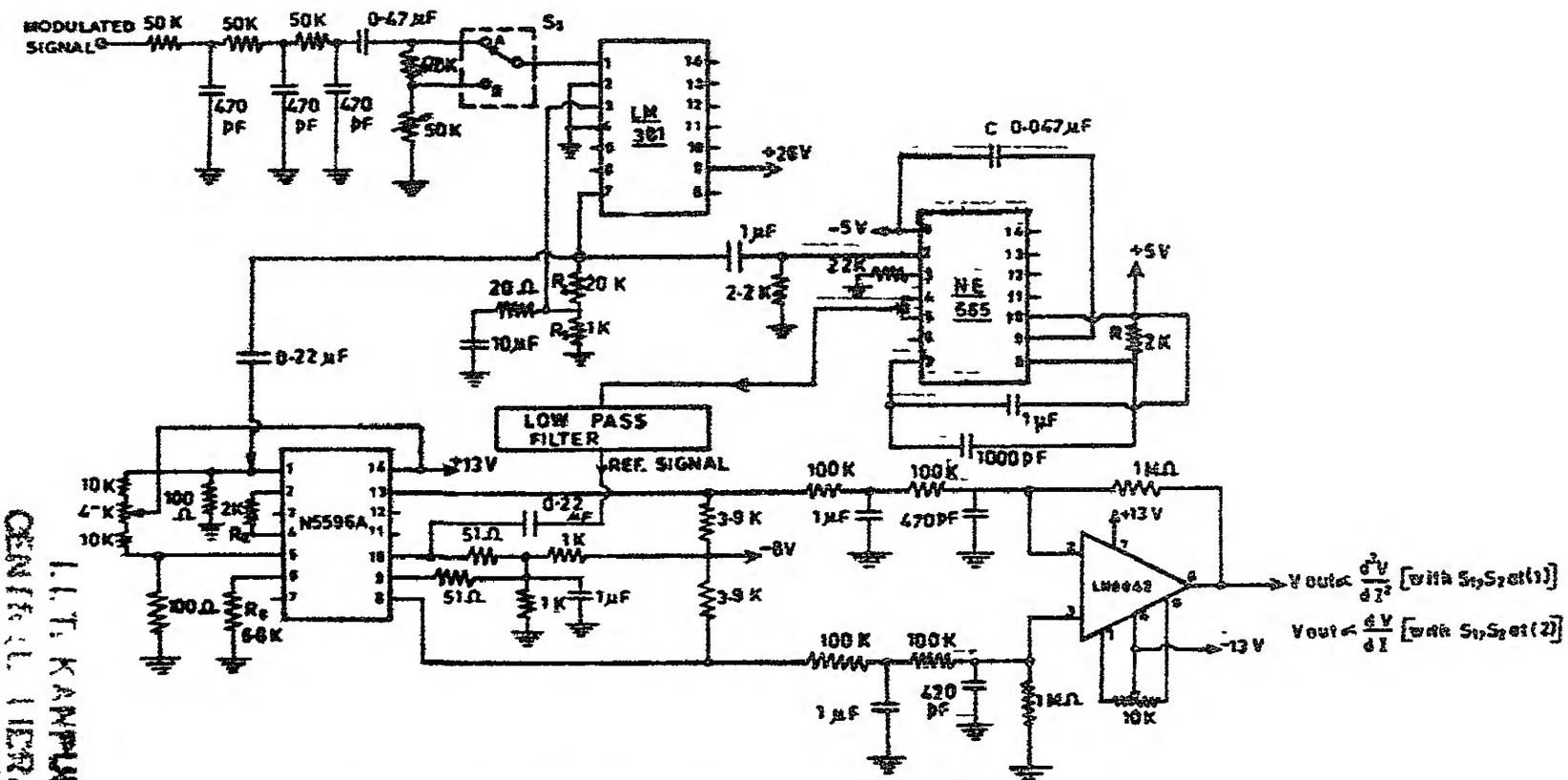

FIG. 12 CIRCUIT DIAGRAM FOR SYNCHRONOUS DETECTION

$$\text{Capture range } f_c = \pm \frac{1}{2\pi} \left(\frac{2\pi f_L}{\tau}\right)^{\frac{1}{2}} \qquad (31)$$

where, $\tau = (3.6).(10^3).C_2$

(here R_1 is in ohm and C_1, C_2 are in farads.)

Using relations (29) to (31) the values of the components, required, have been decided as follows.

$C_1 = 0.047 \ \mu f$

$C_2 = 1.0 \ \mu f$

$R_1 = 2 \ K \ \Omega$

A capacitor of 0.001 μf connected between pins 7 and 8 suppresses oscillation in the control current source of PLL.

The small α low pass filter required to filter out the odd harmonics from the phase locked square wave output of VCO has already been discussed in Section 4.2.1. The sinusoidal signal thus obtained is used as a reference frequency signal for synchronous detection for getting voltages proportional to both $I(dV/dI)$ and $-I^2(d^2V/DI^2)$. Moreover, it is also used as the modulating signal for getting the voltage proportional to $I(dV/dI)$.

4.3.4 Detector:

If $e_1 = E_1 \cos \omega_1 t$ and $e_2 = E_2 \cos(\omega_1 t + \phi)$ be the two voltages fed to the input of the balanced demodulator, the output voltage e_o is given by

$$e_o = A_V\, e_1 e_2 = A_V \cdot \frac{E_1 E_2}{2} \{\cos\phi + \cos(2\omega_1 t + \phi)\} \qquad (32)$$

Addition of a simple low pass filter will remove the ac terms and will provide dc voltage given by

$$e_o = A_V \frac{E_1 E_2}{2} \cos\phi \qquad (33)$$

If the two inputs be the same in phase and frequency, the output is simply

$$e_o = \left(\frac{A_V E_1}{2}\right) E_2 \qquad (34)$$

In our case the two inputs to the balanced demodulator are the reference signal and signal proportional to the desired derivative, the former being of fixed amplitude and the latter is dependent on the slope of the device characteristics. Thus

$$e_o = \frac{x\, d^n V}{dI^n} \text{ (x being a constant)} \qquad (35)$$

The N5596A[31] is a double balanced modulator-demodulator which produces an output voltage proportional to the product of an input (signal) voltage and a switching (carrier) signal. It has adjustable gain and signal handling capability, fully balanced inputs and outputs, low offset and drift, wide frequency response upto 100 MHz and excellent carrier suppression (typically 60 db).

The upper quad differential amplifier as well as the lower differential amplifier are operated in a linear mode. The output signal will thus contain the sum and difference frequency terms. The sum frequency term is to be filtered out and since the phase difference of the two incoming signals as well as the reference frequency signal amplitude are maintained to be constant, the difference frequency term i.e. a dc voltage will vary in accordance with the variation of the difference frequency signal amplitude.

In order to avoid the saturation of the upper port the signal amplitude must be less than 60 mV_{rms}, and hence it is obvious that the reference frequency signal should be fed at the upper port since its amplitude is fixed and it is the difference frequency signal which should be fed to the lower port because its linear variation is of interest.

For linear operation, the derivative signal $e_2 = E_2 \cos \omega t$ should follow:

$$E_2 \leq I_6 R_E \quad \text{(volts peak)} \tag{36}$$

and the voltage gain is given by

$$A_V = \frac{R_L V_{c(rms)}}{2\sqrt{2}\left(\frac{kT}{q}\right)(R_E + 2r_e)} \quad \text{(for single ended output)} \tag{37}$$

where, I_6 = the bias current (≤ 10 mA)

R_E = gain adjust resistance

R_L = load resistance

and $r_e = \frac{26\ mV}{I_6(mA)}$ (38)

The gain adjust resistance is given by

$$R_5 = \left(\frac{V^- - 0.75}{I_6} - 500 \right) \text{ ohm} \quad (39)$$

It is usually assumed that $I_6 = I_8 = I_{13}$, so that the common mode quiscent output voltage is related as

$$V_8 = V_{13} = V^+ - I_6 R_L \quad (40)$$

The N5596A requires three dc bias voltage levels which must be set externally, guidelines include maintaining at least 2 volts collector base bias on all transistors while not exceeding the maximum voltages specified.

The restrictions imposed may be summarized as:

$$\begin{aligned} 30\ V_{dc} &\geq (V_8, V_{13}) - (V_9, V_{10}) \geq 2\ V_{dc} \\ 30\ V_{dc} &\geq (V_9, V_{10}) - (V_1, V_5) \geq 2.7\ V_{dc} \\ 30\ V_{dc} &\geq (V_1, V_5) - (V_6) \geq 2.7\ V_{dc} \end{aligned} \quad (41)$$

The design steps are given below:

Let I_6 be 1.0 mA, so that $r_e = 20\ \Omega$ from expression (38). Since $I_2 < 2^{\vee}$, from restriction imposed by relation (36)

$$I_6 R_E \geq 2.0 \text{ V}$$

or $$1.0 R_E(\text{K}\Omega) \geq 2.0\text{V}$$

For a differential output connection, gain

$$A_V = \frac{R_L V_c \text{ (rms)}}{2\sqrt{2}\left(\frac{kT}{q}\right)(R_E+2r_e)} \qquad (42)$$

Thus the maximum output voltage (peak)

$$= I_6 R_L = 1.0 R_L \text{ (K}\Omega\text{)}$$

$$\simeq \left[\frac{1.0\ R_L(\text{K}\Omega)}{R_E\ \ (\text{K}\Omega)}\right]\times 2 \quad V_{peak} \qquad (43)$$

From relations (42) and (43) R_L = 5.9 KΩ and R_E = 2 KΩ is a good choice.

(b) $$R_5 = \left(\frac{V^- - 0.75}{I_5} - 500\right) \text{ ohm}$$

$$= \left(\frac{8 - 0.75}{1.0\text{x}10^{-3}} - 500\right) \text{ ohm}$$

$$= 6.8 \text{ K-ohm}$$

(c) Within the restriction by equations (41) the biasing resistors are calculated and shown in Figure 9.

(d) Carrier null is achieved by means of a bias trim potentiometer R_1 shown.

(e) A simple RC filter is connected at both the output pins to filter out the second harmonic produced due to

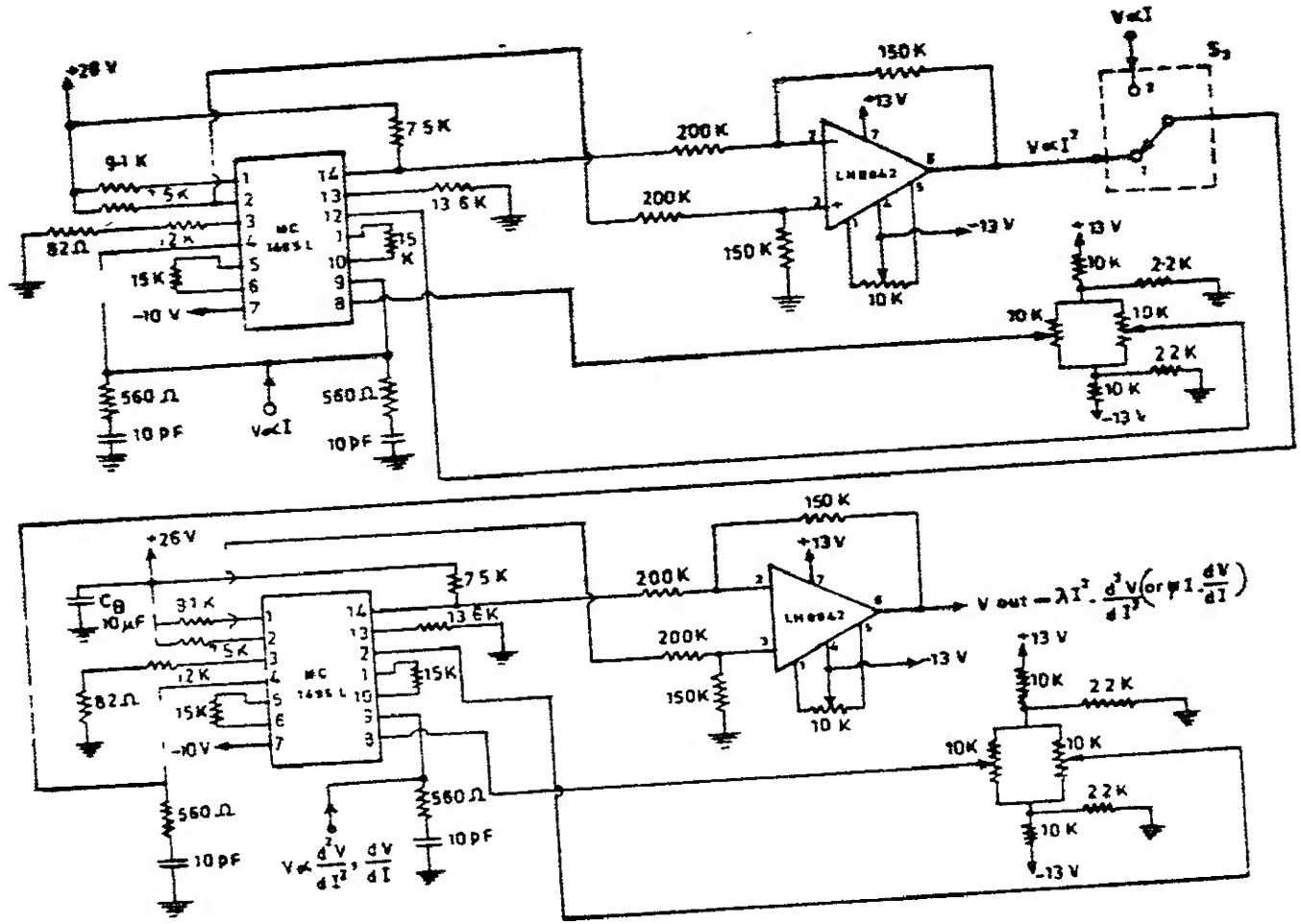

FIG. 13 CIRCUIT DIAGRAM FOR ANALOG MULTIPLICATION

multiplication and third and fifth harmonic due to over driving the upper differential amplifier.

(f) A high input impedance opamp (LH0042) has been used to convert the balanced output into a single ended one.

4.4 Analog Multiplication

So far the system design to get dV/dI, d^2V/dI^2 and $V \propto I$ has been discussed. Our aim is to get $I(dV/dI)$ and $-I^2(d^2V/dI^2)$. The first will need only one analog multiplier while the latter the two.

The MC1495L[31] is a monolithic four quadrant multiplier designed for uses where the output voltage is a linear product of two input voltages. It has excellent linearity (2% max. error on X input, 4% max. error on Y input), adjustable scale gain factor(Z) excellent temperature stability and wide input voltage range ($\pm$10V). It is quite suitable for our purpose.

Sources of Multiplier Error:

The major source of error in the multiplier arises from voltage offsets and ohmic base resistances in the four output transistors and base diodes. A second and usually small source of error can arise from large signal nonlinearity in the X and Y input differential amplifiers. Care must be taken to avoid aging and temperature drift in the external - components used

with the multiplier. The last one has been avoided by using precision components in the level translation circuitry. To avoid introducing error from the second source, the emitter degeneration resistors R_x and R_y have been chosen large enough so that nonlinear base emitter voltage variation can be ignored.

For small inputs, the differential output voltage for a typical unadjusted multiplier may be written as.

$$V_{out} = Z(V_x \pm \phi_x \pm V_{x\ offset})(V_y \pm \phi_y \pm V_{y\ offset}) \pm V_{o\ offset} \qquad (44)$$

where, ϕ_x = equivalent X input offset term

ϕ_y = equivalent Y input offset term

$V_{o\ offset}$ = output offset that remains after the inputs are zeroed.

Thus first X and Y Inputs are to be zeroed by setting $V_{x\ offset} = -\phi_x$ and $V_{y\ offset} = -\phi_y$. Next $V_{o\ offset}$ is removed by an output adjustment and Z is adjusted for the correct gain.

The circuit for offset adjustment has also been shown in Figure 12.

The differential output voltage of the multiplier is given by

$$V_{out} = V_{O1} - V_{O2} = \frac{2V_x V_y R_L}{I_3(R_x + \frac{2kT}{qI_{13}})(R_y + \frac{2kT}{qI_3})} = Z(V_x V_y) \qquad (45)$$

where kT/q = 26 mV at 25°C. The scale factor Z can be adjusted with a suitable choice of I_3, R_x, R_y and R_L.

(a) Due to power dissipation limitation I_{13} and I_3 are kept below 2.0 mA. Here they have been chosen 0.65 mA and 0.75 mA respectively. The restriction on input signal handling capability is given by

$$\begin{aligned} V_{x(max)} &< I_{13}R_x \\ V_{y(max)} &< I_3 R_y \end{aligned} \qquad (46)$$

Thus for $V_{x(max)} = V_{y(max)} = 10$ V

$$R_x = R_y > 10 \text{ K}\Omega$$

In order to insure that $R_x >> \frac{kT}{qI_{13}}$ and $R_y >> \frac{kT}{qI_3}$ even with maximum input voltage, let $R_x = R_y = 15$ K Ω.

(b) For Z = 2/15, the value of R_L is calculated to be

$$\begin{aligned} R_L &= \frac{Z}{2} I_3 R_x R_y \\ &= \frac{1}{2}\left(\frac{2}{15}\right)\left(\frac{3}{4} \times 10^{-3}\right)(15 \times 10^3)(15 \times 10^3) \\ &= 11.25 \text{ K}\Omega \end{aligned}$$

(c) From the curve in the concerned data book (ref. 31), for an input swing of ±10V, voltage V_1 may have a minimum value of +12V. (This minimum V_1 is approximately two forward diode drops above $V_{x\,max}$ and one diode

drops above $V_{y\ max}$). With a 1.5V safety margin, V_1 becomes 13.5 V.

Then the positive supply is given by

$$V^+ = V_1 + \{\frac{Z\ V_{x(max)}\ V_{y(max)}}{2}\} + I_{13}R_L \qquad (47)$$

On substitution,

$$V^+ = 13.5 + (2/15)(1/2)(10)(10) + (0.65\times10^{-3})(11.25\times10^{3})$$

$$\approx 26V$$

(d) Value of R_1 is given by

$$R_1 = \frac{V^+ - V_1}{2I_3} \qquad (48)$$

On substitution,

$$R_1 = \frac{26 - 13.3}{(2)(0.75)} \text{ K-ohm}$$

$$= 9.1 \text{ K-ohm}$$

(e) The negative voltage is selected to be -10V based on the fact that with the maximum positive input voltage applied, the maximum voltage between the input and the negative supply does not exceed the 30V breakdown limit.

(f) The current I_{13} and I_3 have been set by means of dropping resistors from ground to pins 13 and 3 respectively, whereas,

(iii) +5V

(iv) +26V

Conventional approach with rectification, filteration, voltage regulation and provision of tracking for symmetric voltages has been employed. The voltages other than above are obtained using Zener diodes.

CHAPTER 5

ADVANTAGEOUS FEATURES OF THE SYSTEM

In Chapter 2, it has been discussed that the "Dual-frequency technique" had a number of desirable features as compared to the other ones. It was developed by Taoli and Svacek[16] and commercial equipments were used by them to get various derivatives. It was felt that an instrument would be even more useful if it can be made small, compact and less expensive by dispensing with general purpose commercial equipment and building specific hardware to meet the specific function. Obviously the main advantages of the present system are low cost, small size, optimum performance, good resolution and the simplicity of operation. These features have been discussed in the following paragraphs.

Low cost:

Since for the "Dual-frequency technique" the prime necessity is a frequency generator capable of providing a single fixed frequency(with stability better than 20 ppm/°C) there is no need to use a variable frequency oscillator. Hence in the present system the oscillator is made by using a comparator μA710, and a stable quartz crystal.

For frequency multiplication Taoli and Svacek used a commercial selective amplifier and obtained the nth

harmonic of the input frequency. The function of this equipment has been replaced by a PLL XR215, a counter SN7490, and logic gate SN7400.

A voltage regulator chip μA723 with transistor 2N3053 has provided a constant current source with an obvious substitution for an equipment with the same function.

The special achievement of the structure is the replacement of a costly equipment named Lock-in amplifier. No doubt the latter has several good features like a very high gain of the order of 10^4, a precision attenuator, a good selective amplifier with Q of the order of 25, a variable range phase shifter etc. Since in the present method, the phase detection is to be done at a single frequency, the meritorious features of it can be conveniently obtained using modern ICs. Most of these merits have been achieved though with less precision but adequate for our purpose in the present system. A low noise pre-amplifier LM381 has been used to provide a gain of 1000. A PLL NE565 has been used to provide the reference frequency, signal with the same phase as that of the difference frequency signal. Here one outstanding feature is that the phase adjustment is automatic as compared to the manual one in Lock-in amplifier. The synchronous detection is achieved by using a balanced modulator chip N5596A.

The function of the equipment PAR multiplier has been served by an IC MC1495L, an analog multiplier.

Thus, one can very well compare the total cost of the present system with that of the sum of the cost of the expensive equipments used previously. A large reduction in the cost of the system developed may enable it to be used in Laboratories as a good tool for derivative measurements.

Small size:

The hardware consists of only five P.C.boards with a transformer, attenuators and multiturn potentiometers. Thus a compact small size is achieved.

Optimum performance

The best possible active and passive components have been used. The frequency stability of the two modulating frequencies is of the same order as that from a crystal itself. The active low pass filters used are the low sensitive filters[25,26]. The distortion level of the sinusoidal frequencies obtained after these filters is less than 0.1%. For preamplification a low noise amplifier IM381, with total noise voltage less than 0.5 μV_{rms} was used. The balanced modulator-demodulator N5596A used for synchronous detection has fully balanced inputs and outputs, low offset voltage and small drift with temperature. The multipliers MC1495L have been adjusted for the least

possible offsets. Wherever preferred the 0.1% and 1% metal film resistors, silver-mica and polyster capacitors were used so as to provide the optimum performance.

Good resolution

The modulating constant ac currents are kept sufficiently small as compared to the bias current I_o to provide better resolution. Using multiturn potentiometers, the bias current could be varied with the resolution of better than 0.01 mA.

Simplicity of operation

The only external controls kept, are the attenuator controls and the bias current controls, hence even a non-technical person can easily operate the system.

CHAPTER 6

DEVICE CHARACTERIZATION

Let us first of all consider p-n junction diodes. The total current in the forward direction for the voltages greater than a few tenth of a volt can be written as

$$I = I_s e^{V/V_T} + I_{Ro} e^{V/2V_T} \qquad (49)$$

where I_s = diffusion current constant

and I_{Ro} = generation-recombination current constant.

For Ge p-n junctions the second term is small except at very low temperatures and the ideal diode law is obeyed. For Si p-n junctions the constant I_s is small compared to I_{Ro} except at high temperatures in excess of 150°C and the diode current increases as $e^{V/2V_T}$ upto a voltage of the order of half of a volt. As V is increased further the first term in equation (49) becomes larger compared to the second term and the current starts increasing as e^{V/V_T}. This remains true only upto the time the current is not so large that the voltage drop across the bulk semiconductor and ohmic contacts i.e. the ohmic voltage drop, becomes comparable to the voltage dropped across the space-charge layer. In case, the ohmic voltage drop becomes large, the I-V relation gets modified to

$$I = I_s \exp\left(\frac{V-IR}{V_T}\right) \qquad (50)$$

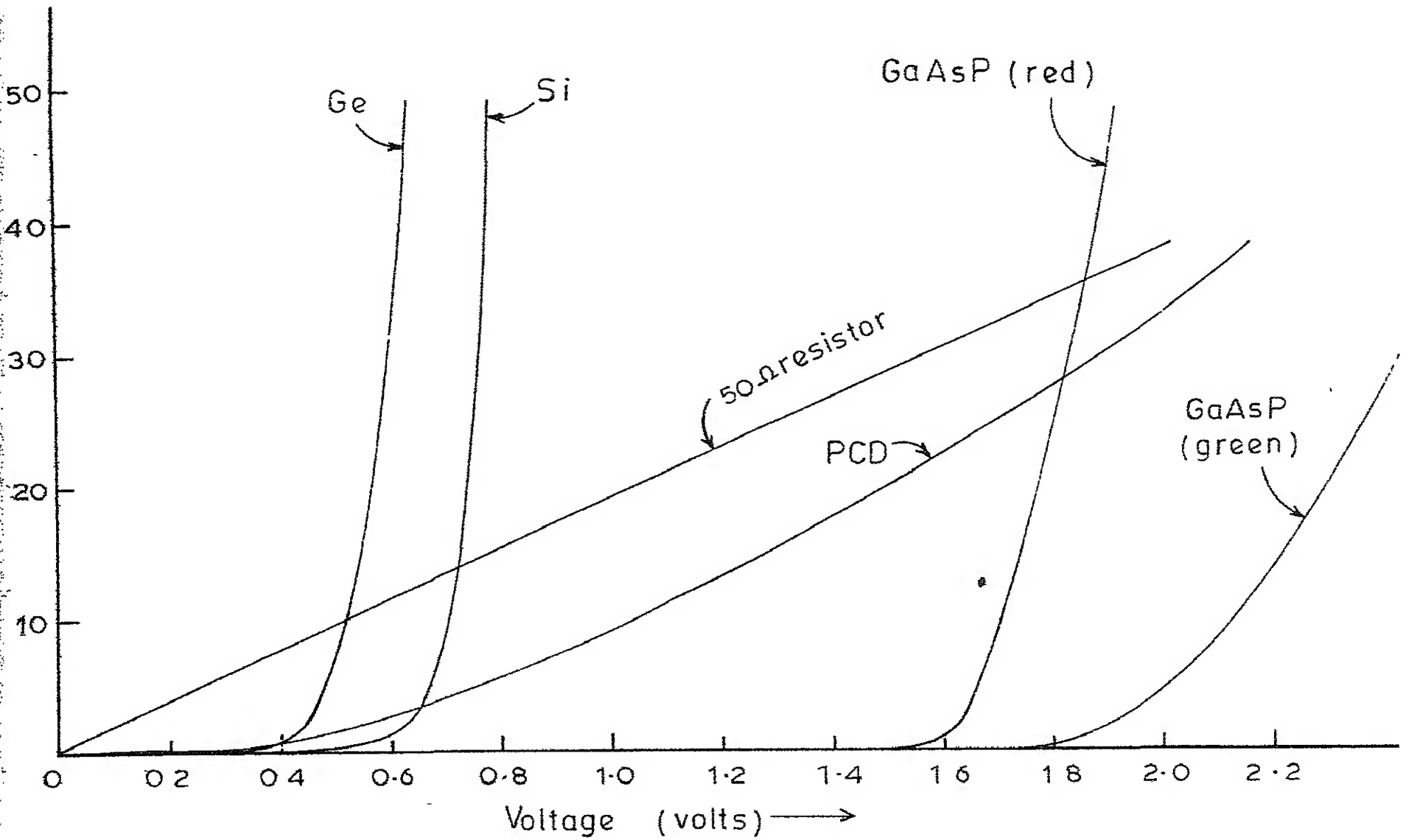

Fig. 14 I–V characteristics of a few junction devices

In most of the modern day diodes, the value of R is quite small (of the order of a few ohms) and the transition from the exponential to the linear region occurs at very large currents. At such large currents the limit of low level injection is exceeded and the injected minority concentration at least in one of the neutral region becomes comparable with the majority carrier concentration in that region. This has two implications. Firstly, the excess injected carriers modulate the conductivity of the neutral regions so that the series resistance decreases with increasing current. Secondly, at large injection conditions the above low level injection treatment is not valid and nonlinear effects set in. For these reason the potential drop across the neutral regions at high currents is not related linearly to the diode current. Hence the linear relation between the diode current and the diode voltage is not observed in diodes even at large currents. In the intermediate current range where large injection conditions have not set in but there is a significant voltage drop across the diode series resistance, equation (50) can be used to determine the value of R.

From the above discussion it follows that the current voltage relation of a junction diode can be expressed by

$$I = I_s \left[\exp\left(\frac{V-IR}{\eta V_T}\right) - 1 \right]$$

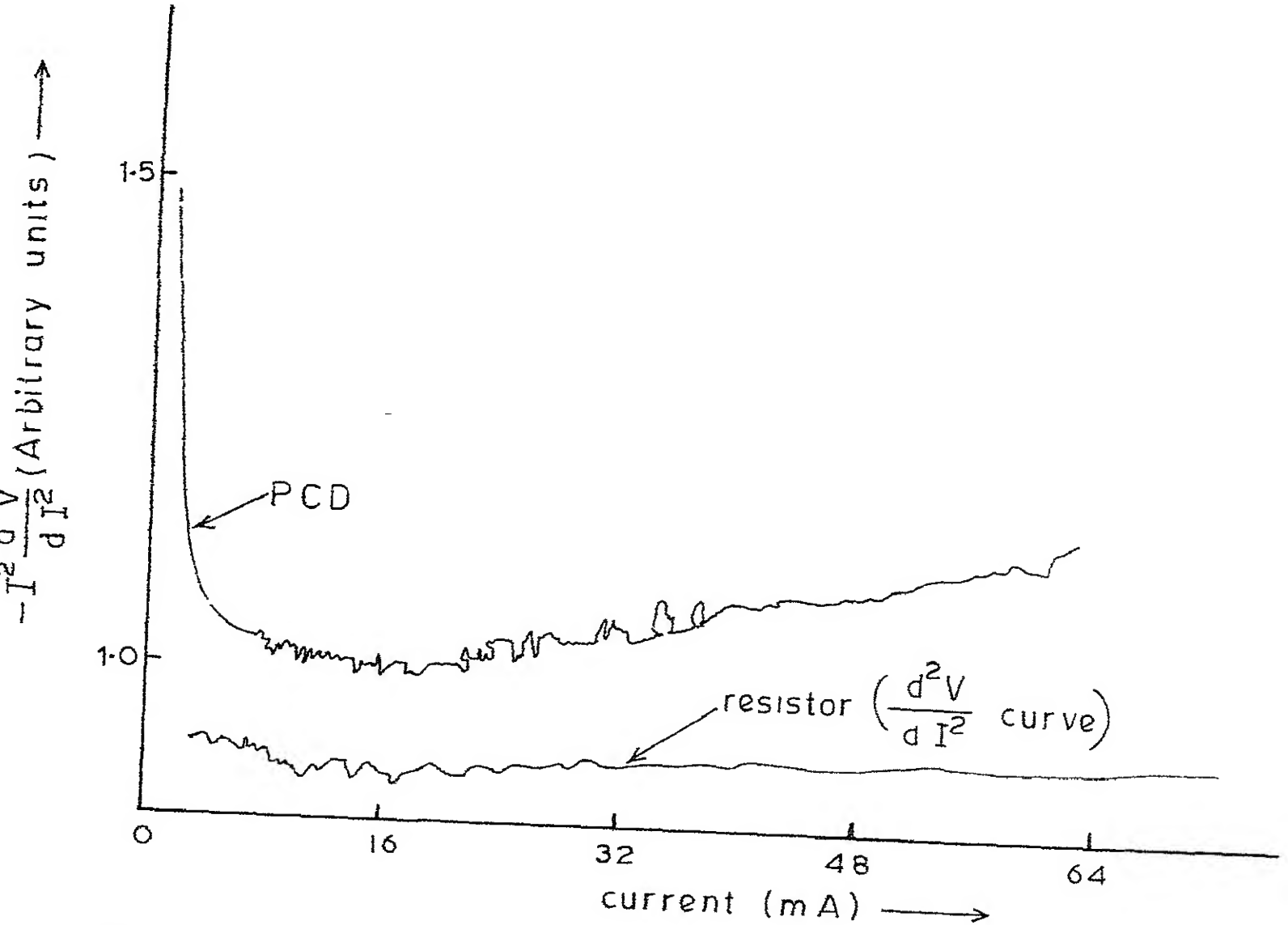

Fig. 15 $\eta - I$ characteristics of a point contact diode (SEM PCD)

where, I_s is determined by the carrier diffusion process and the effect of generation recombination process, is taken into account - by incorporating the factor η .

I-V Characteristics

In Figure 14, the I-V plots of a few devices have been shown. For illustration, a Si diode (1H1), a Ge diode (base to emitter junction of AF115), a point contact diode (SEM ICD), two LEDs (GaAsP) and a 50 ohm (5%, 5W) resistor have been chosen.

From the I-V curves, for Si and Ge diodes the mechanism of current transport is not apparent. Light emitting diodes also show the I-V characteristics similar to those of the ordinary Ge or Si diodes, except that the cut-in voltage V_γ in these cases is higher. Moreover, the threshold point of light emission cannot be decided on the basis of it.

Derivative Characteristics

Resistor:

From the I-V curve, there appears perfect linearity of the resistor, although its second derivative is of a non-zero value. The purpose of choosing a resistor here is to show the sensitivity of the system to even a small nonlinearity. From the second derivative it is clear that the I-V relation for the resistor used is

$$I = a_1 V + a_2 V^2$$

where $a_1 = 1/50$ and a_2, though very small is clearly effective in exhibiting the nonlinearity.

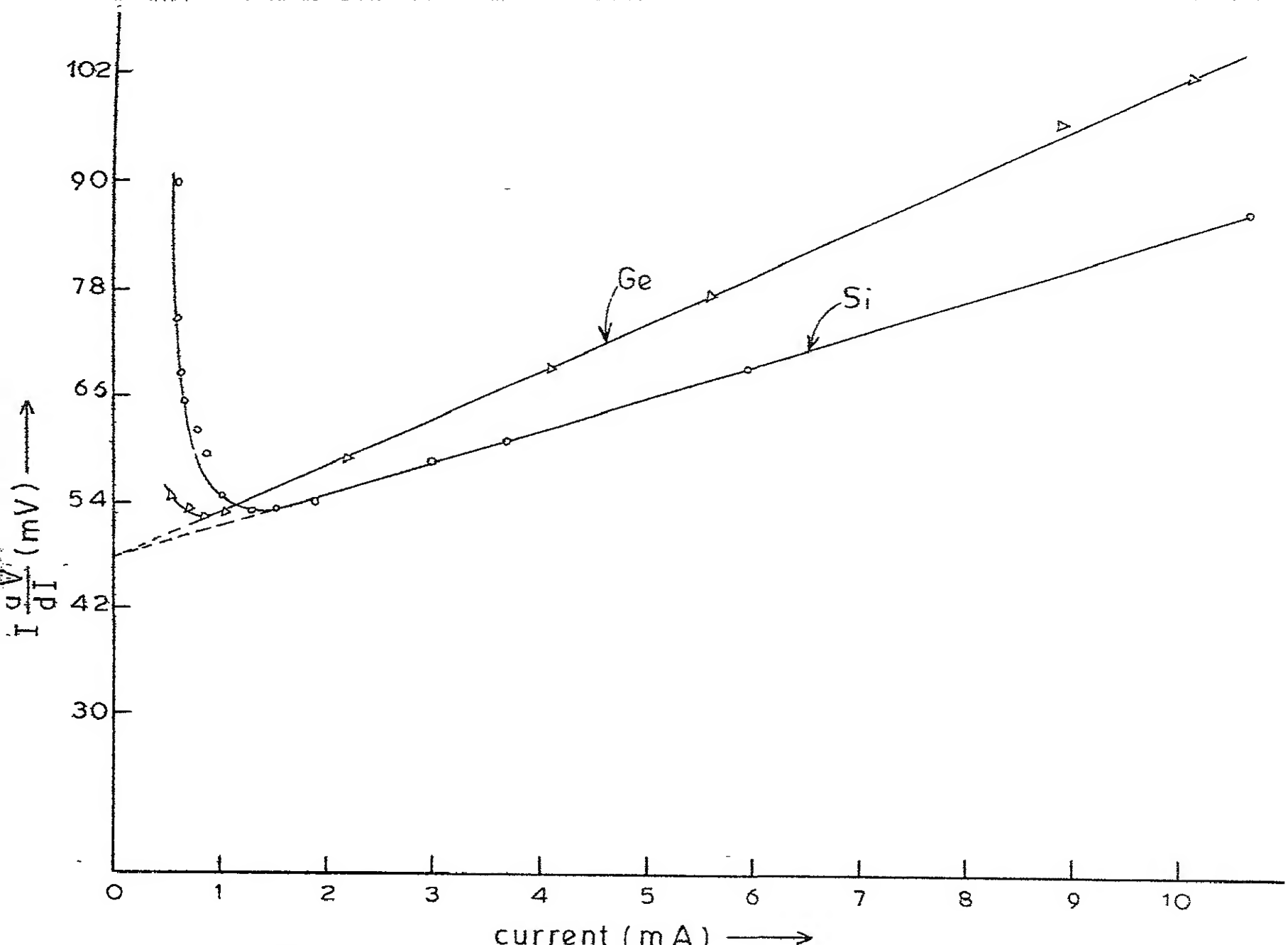

Fig. 16 $I\frac{dV}{dI}$ vs I characteristics of a Si($1H_1$) and a Ge (B-E junction of AF 115) diode.

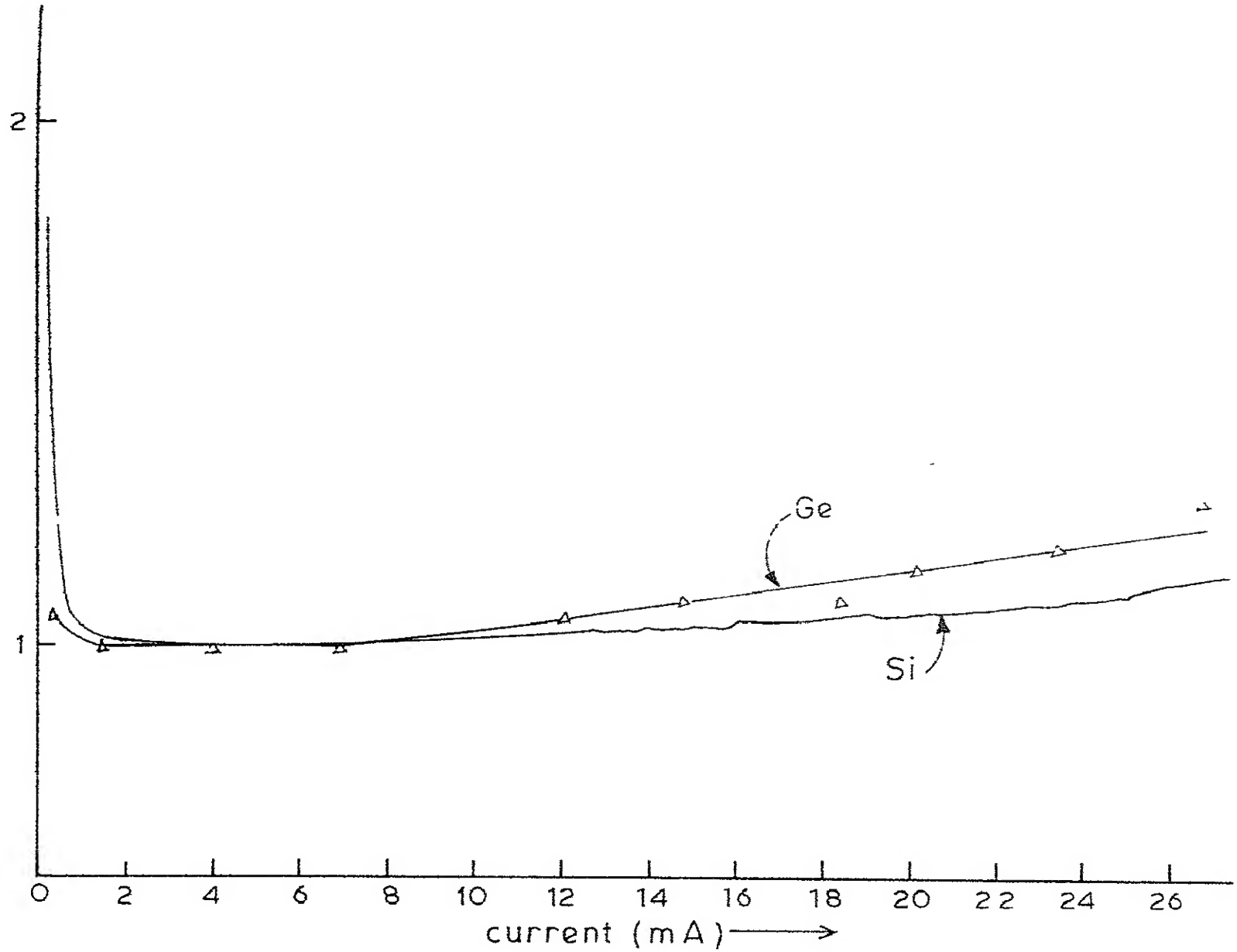

Fig.17 η–I characteristics of a Si (1 H1) and a Ge(B-E junction of AF 115)diode

Point Contact Diode (PCD)

The $-I^2 \frac{d^2V}{dI^2}$ versus I characteristic of diode SEM PCD has been shown in Figure 15. The value of η is greater than unity in the beginning as well as at higher currents. The value of η is approximately unity in region between 10 to 16 mA.

Si and Ge diodes

According to equation (10), the $I \frac{dV}{dI}$ versus I curves represent the series resistance R by the slopes to x axis, and the η by the intercepts on the y axis.

From Figure 16, the series resistance R of the Si diode IN1 is approximately 3.8 ohm. For base to emitter junction of the Ge transistor (AF115) the value of the series resistance is found out to be 5.3 ohm. The intercepts to y axis are approximately the same for the two curves and correspond to $\eta = 1$.

In Figure 17, the three regions; where,(i) η varies from 2 to 1 (ii) $\eta = 1$ and (iii) $\eta > 1$ due to series resistance are clearly visible for Si, whereas the absence of the first region confirms that the diffusion current in Ge is always sufficiently greater as compared to the generation recombination current.

LEDs

From the slope of the curves for Green and Red LEDs as shown in Figure 18, the series resistances are found out to be 9 ohm and 5.3 ohm respectively.

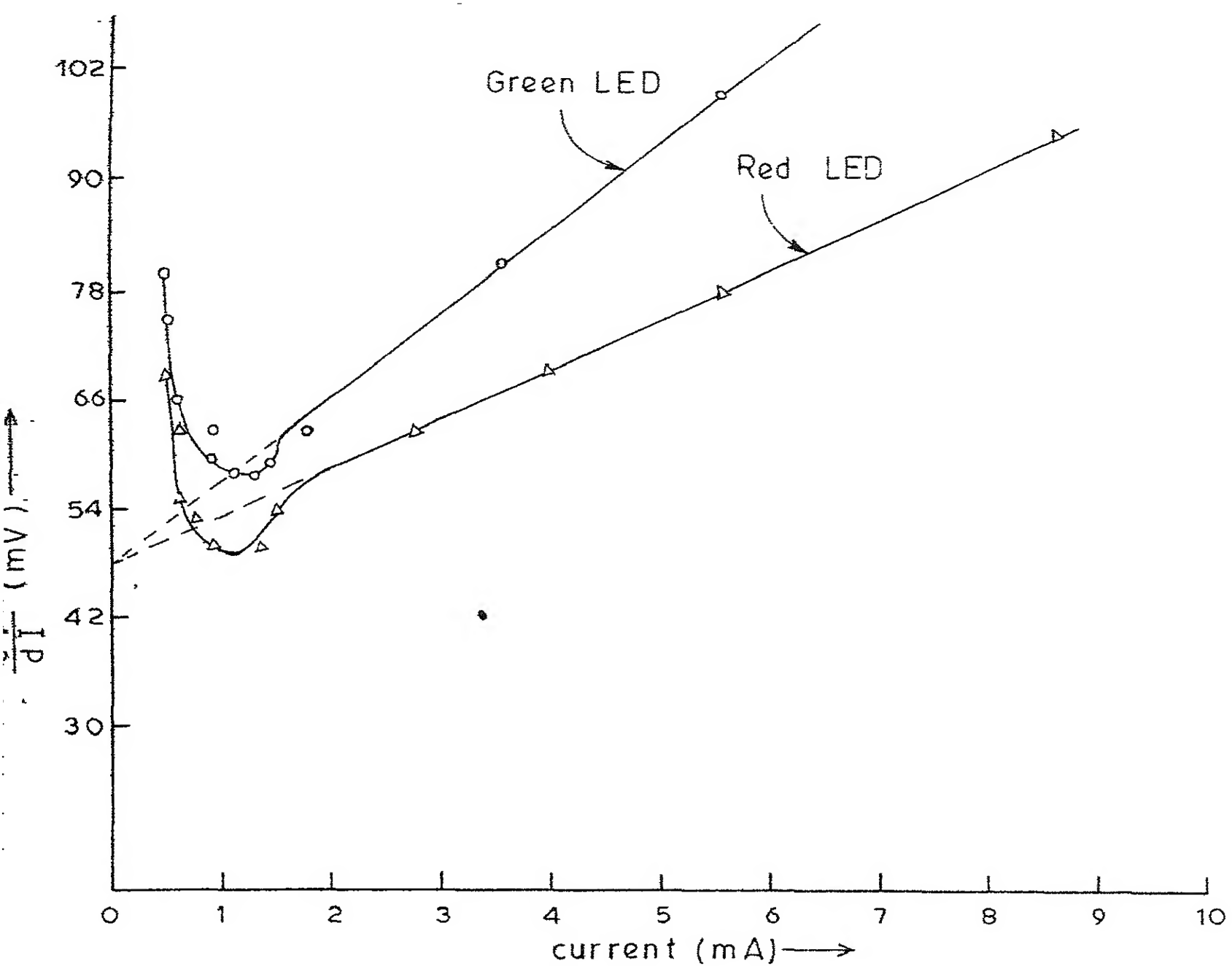

Fig. 18 $I\frac{dV}{dI}$ vs I characteristics of red and green LEDs (GaAsP)

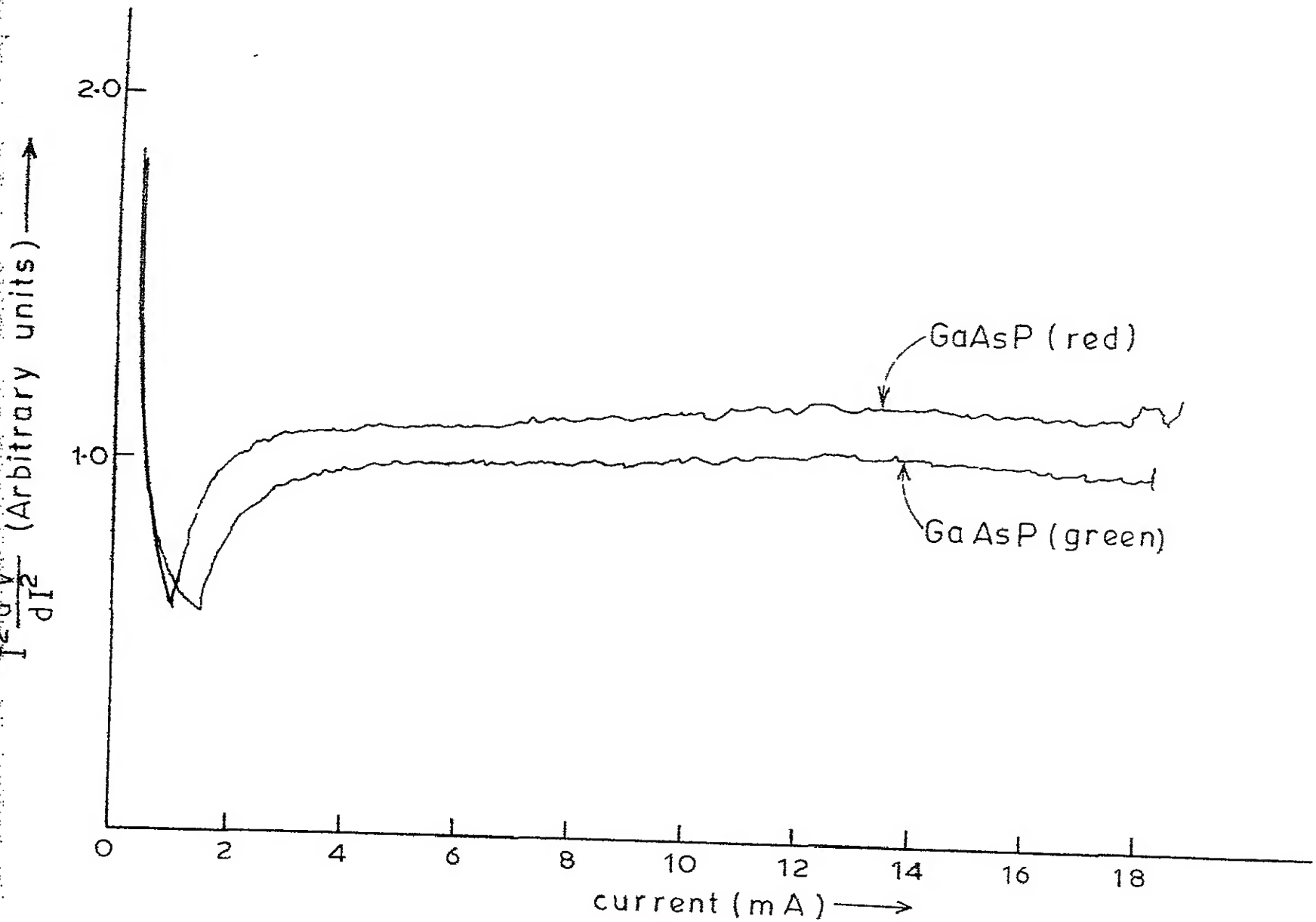

Fig 19 $\eta - I$ characteristics of red and green LEDs (GaAsP)

Particularly strong indications of the light emission process is contained in the second derivative response, which is due to the saturation of the junction voltage at the onset of light emission. For green and red LEDs the currents at the threshold points are 1.5 mA and 1 mA respectively, which have the same values as shown by the first derivatives. The corresponding voltages at these points are 1.88 volts and 1.6 volts respectively.

REFERENCES

1. R.N. Hall, J.H.Racette and H.Ehrenreich, "Direct observation of polarons and phonons during tunneling in group 3-5 semiconductor junctions", Physics Review Letters, Vol.4, p. 456 (1960).

2. J.J. Tieman, "Automatic conductivity plotting machine", Review of Scientific Instruments, Vol.32, p. 1093 (1961).

3. A.G.Chynoweth, R.A. Logan and D.E. Thomas, "Derivative measurement for tunneling junctions", Physical Review, Vol.125, p. 877, (1961).

4. J.G. Adler and J.E. Jackson, "System for observing small nonlinearities in tunnel junctions", Review of Scientific Instruments, Vol.37, p.1079 (1966).

5. J.M.Rowell, W.L. McMillan and W.L.Feldmann, "Phonon emission and self energy effects in Normal metal tunneling", Physical Review, Vol.180, p. 658 (1969).

6. R.C. Jaklevic and J. Lambe, "Molecular Vibration spectra by electron tunneling", Physics Review Letters, Vol.17, p. 1139 (1966).

7. R.W. Dixon, "Derivative measurement of light current-voltage characteristics of (Al,Ga)As double heterostructure lasers", The Bell System Technical Journal, Vol.55, p.973 (1976).

8. T.L. Paoli, "Observation of second derivatives of the electrical characteristics of double-hetrostructure junction lasers", IEEE Transactions on Electron Devices, Vol. ED-23, No.12, p. 1333,(1976).

9. T.L. Paoli and P.A. Barnes, "Saturation of the junction voltage in scripe-geometry (AlGa)As double-hetrostructure junction lasers", Applied Physics Letters, Vol.28, p. 714 (1976).

10. J.A. Barnes and Thomas L. Paoli, "Derivative measurement of the current-voltage characteristics of double hetrostructure injection lasers", IEEE Journal of Quantum Electronics, Vol.12, p.633 (1976).

11. A.N. Saxena, "Forward I-V characteristics of Schottky barriers on n-type silicon", Surface Science 13, p. 151-171, (1969).

12. R.V. Coleman, R.C. Morris and J.E. Christopher, Methods of Experimental Physics, Vol.II, Academic Press, New York, p. 163 (1974).

13. J.S. Rogers, "Conductance Bridge for Electron Tunneling Measurements", Review of Scientific Instruments", Vol.41, p. 1184,(1970).

14. H.W. Korb and N. Holonyak, Jr., "Measurement system for derivative studies", Review of Scientific Instruments, Vol.43, p.90, (1972).

15. J.G. Adler, T.T. Chen and J. Strous, "High resolution Electron tunneling spectroscopy", Review of Scientific Instruments, Vol.42, p. 362 (1971).

16. T.L. Pioli and Joseph F.Svacek, "Derivative measurement by frequency mixing", Review of Scientific Instruments, Vol.47, p. 1016, (1976).

17. D.E. Thomas and J.M. Klein, "Tunneling current structure resolution by differentiation", Review of Scientific Instruments, Vol.34, p. 920(1963).

18. William R. Patterson and J. Schewchun, "Alternate approach to the resolution of tunneling current structure by differentiation; Review of Scientific Instruments, vol.35, p. 1704, (1964).

19. W.R. Patterson, III and M.Kuhn, "An electronic system for measuring the electrical characteristics of non-linear devices", Review of Scientific Instruments, Vol.40, p.960, (1969).

20. S.K. Mitra, Analysis and Synthesis of Linear Active Circuits, John Wiley and Sons, Inc., New York, p.19, (1969).

21. Tobey, Graeme and Huelsman, Operational Amplifiers, Design and Applications, McGraw-Hill, Kogakusha Ltd., (1971).

22. Jergald, G. Graeme, Applications of Operational Amplifiers, McGraw-Hill, Kogaskusha Ltd., (1973).

23. Davis F. Stout, Milton Kaufman, Handbook of Operational Amplifier Circuit Design, McGraw-Hill,(1976).

24. Coughlin and Driscoll, Operational Amplifiers and Linear ICs, Prentice Hall, (1976).

25. K. Radhakrishna Rao and S.Venkateswaran, "Active RC synthesis of driving impedances", Journal of the Institution of Telecomm.Engg., Vol.17, No.10, p.365, (1971).

26. M.A. Soderstrand and S.K.Mitra, "Extremely low sensitivity active filters", Proc. of IEEE, Vol.57, p. 2175 (1969).

27. Linear IC Data Book, Exar Integrated Systems Inc.,(1972)

28. Linear Data Book, National Semiconductor Corp., (1976).

29. Fairchild Semiconductor Integrated Circuit Data Catalog, Fairchild Semiconductor,(1970).

30. Marvin K. Vander Kooi,"Linear Applications," Vol.I, National Semiconductor Corp.,(1976).

31. Linear Integrated Circuit Data Book, Motorola Inc. (1971).

32. Signetics Data Book; Signetics Corporation (1974).

33. Joseph Lindmayer, Charles Wrigley, Fundamentals of Semiconductor Devices, Van Nostrand Reinhold, East West Press,(1965)

34. Frederick F. Driscoll, Robert F. Coughlin, Solid State Devices and Applications, Prentice Hall,Inc., (1975).

35. S.M.Sze, Physics of Semiconductor Devices, John Wiley & Sons, Inc., (1969).

APPENDIX 1

EFFECT OF PARAMETER VARIATIONS ON THE DERIVATIVES*

The assumptions of $\frac{\eta kT}{q}$, R and I_s as independent of current may sometimes be unjustified. If $1/\beta = \eta kT/q$ depends on current through the parameter η, the first order correction to the derived value of η is,

$$\Delta\eta\,(I) = \frac{1}{V_T}(V-IR)\,\frac{I}{\eta}\,\frac{d\eta}{dI} \qquad (A.1)$$

This correction can be large for quite reasonable I-V characteristics. Equivalently one finds instead of previous equation (10) used in Chapter 3:

$$I\,\frac{dV}{dI} = \eta\,V_T + \frac{V}{\eta}\,\frac{d\eta}{dI} + IR\left(1 - \frac{I}{\eta}\,\frac{d\eta}{dI}\right) \qquad (A.2)$$

Thus, both of the derived parameters $\eta\,V_T$ and R_s are sensitive to the assumption of $1/\beta$, independent of current.

Analogous comments apply in the second derivative case where one may have

$$I^2\,\frac{d^2V}{DI^2} = -\eta\,V_T\left(1 - \frac{2I}{\eta}\,\frac{d\eta}{dI}\right) + (V - IR_s)\,\frac{I^2}{\eta}\,\frac{d^2\eta}{dI^2} \qquad (A.3)$$

Similarly, the equations when $R = R(I)$ and $I_s = I_s(I)$ can be easily derived.

---

* R.W. Dixon - Derivative Measurement of Light Current Voltage Characteristics of (Al,Ga)As Double Heterostructure Lasers; The Bell System Technical Journal, Vol. 55, p. 973, (1976).

APPENDIX 2

HIGHER ORDER DERIVATIVES**

Although the dual frequency technique had been used for second order derivative, the same approach is applicable to measurements of the derivatives with order higher than two. A third derivative is sensed by a component at the 'difference' frequency $f = f_2-(f_1-f_2)$. For this case, the appropriate selection of frequencies is determined by requiring f to be the lowest frequency in the device response and the next lowest frequency (f_1-f_2), to be n times as large as f. All other frequencies generated by terms of order 3 or lower are generated than nf itself. The appropriate modulation frequencies for the third derivative measurement are $f_1 = (2n+1)f$ and $f_2 = (n+1)f$, and the factor n is determined by the ability of the available electronics to eliminate feedthrough of the strong signals at f_1, f_2 and f_1-f_2.

Similarly, a fourth derivative is sensed at the difference frequency $f = f_2-(f_1-2f_2)$ and f_1-2f_2 is taken to be n times f. The appropriate modulation frequencies

---

** T.L. Paoli and Joseph F. Svacek - Derivative Measurement by Frequency Mixing; Reviewof Scientific Instruments, Vol.47, p. 1016, (1976).

for detection of a fourth derivative are then $f_1=(3^n+2)f$ and $f_2 = (n+1)f$.

This selection process can be generalized to the **mth** derivative with the result that

$$f_1 = \{(m-1)n + (m-2)\}f$$

and $$f_2 = (n+1)f$$

Eventually, the factor n will become prohibitively large.

APPENDIX 3

IMPORTANCE OF THE GAIN OF THE BUFFER IN DECIDING THE PERFORMANCE OF A LOW PASS FILTER

For a low pass filter shown in Figure 9, let the gain of the two buffers be the same and equal to K.

Then if v_o be the output voltage; the voltage v' after the first buffer and v_i the input signal voltage are given by

$$v' = \frac{v_o}{K} + (1 + SC_2 R_2) \qquad (A.4)$$

$$v_i = v_o + (\frac{v'}{K} - v_o)(1 + SC_1 R_1) \qquad (A.5)$$

On substituting v' from equations(A.4) to (A.5), one may get

$$v_i = v_o + \{\frac{v_o}{K^2}(1 + SC_2R_2) - v_o\}(1 + SC_1R_1)$$

$$= v_o [\frac{1}{K^2} + \frac{1}{K^2} S^2 C_1C_2R_1R_2 + S\{\frac{C_2R_2}{K^2} + (\frac{1}{K^2} - 1)GR_1\}] \qquad (A.6)$$

From the above equation, the transfer function is to be obtained as

$$H(s) = v_o/v_i = \frac{1}{S^2 \frac{C_1C_2R_1R_2}{K^2} + S\{\frac{C_2R_2}{K^2} + (\frac{1}{K^2} - 1)C_1R_1\} + \frac{1}{K^2}}$$

$$= \frac{K^2/C_1C_2R_1R_2}{S^2 + S\{\frac{1}{C_1R_1} + (1-K^2).\frac{1}{C_2R_2}\} + \frac{1}{C_1C_2R_1R_2}} \qquad (A.7)$$

Comparing the above equation with that of the standard form of a second order low pass filter, we get

$$f_o(\text{the centre frequency}) = \frac{1}{2\pi\,(C_1C_2R_1R_2)^{\frac{1}{2}}} \qquad (A.8)$$

$$\alpha = \frac{1}{Q}\,(C_2R_2/C_1R_1)^{\frac{1}{2}} + (1-K^2)\,(C_1R_1/C_2R_2)^{\frac{1}{2}} \qquad (A.9)$$

H_o(the low frequency gain)

$$= K^2 \qquad (A.10)$$

and $$H_{f=f_o} = K^2/\alpha \qquad (A.11)$$

Let $(C_2R_2/C_1R_1) = x$, so that α may be rewritten as

$$\alpha = x + \left(\frac{1-K^2}{x}\right)$$

$$= \{\sqrt{x} - (1-K^2)/\sqrt{x}\}^2 + 2(1-K^2) \qquad (A.12)$$

One can very well guess that α will be minimum when the first term is equal to zero, then

$$\alpha_{min} = 2(1-K^2) \qquad (A.13)$$

and $$x = (C_2R_2/C_1R_1) = (1-K^2) \qquad (A.14)$$

From equation (A.13), it is evident that the minimum α is dependent only on the gain of the buffer 'K'. Most of the authors (name of a few were given in Chapter 4) neglected this factor completely and concluded their work with maximum $Q = 1/\alpha$ achievable with their circuits. But

as is clear from equation (A.9), the higher the value of the Q decided, the smaller will be its value practically achievable.

The similar derivations can be obtained for any other circuit using a buffer as its active element.

APPENDIX 4

```
C       A PROGRAMME FOR DETERMINING THE REQUIRED DERIVATIVES
        DIMENSION V(20),I(20),DERIV1(20),DERIV2(20),ETA(20),
       1R(20),DEVICE(20),IDEV(20)
        REAL I,IS,IDEV
   10   CONTINUE
        READ 1,(DEVICE(K),K=1,20)
        PRINT 100
        PRINT 1,(DEVICE(K),K=1,20)
        PRINT 100
        READ 2,IS,VT
        PRINT 3,IS,VT
        PRINT 4
        READ 5,NP
        READ 6,(I(K),K=1,NP)
        READ 6,(V(K),K=1,NP)
        CALL DERIVE(V,I,DERIV1,NP)
        CALL DERIVE(DERIV1,I,DERIV2,NP)
        DO 20 K=1,NP
        ETA(K)=-DERIV2(K)*((I(K)+IS)**2)/VT
        R(K)=(DERIV1(K)-(ETA(K)*VT)/(I(K)+IS))*100.
        IDEV(K)=I(K)*DERIV1(K)
        PRINT 7,K,V(K),I(K),DERIV1(K),DERIV2(K),ETA(K),R(K),IDEV(K)
   20   CONTINUE
        GO TO 10
    1   FORMAT(20A4)
    2   FORMAT(2F8.4)
    3   FORMAT(10X,*IS= *,F8.4,5X,*VT= *,F8.4)
    4   FORMAT(10X,*K*,10X,*V*,10X,*I*,10X,*DV*,10X,*D2V*,10X,
       1*ETA*,10X,*R*,10X,*DV*/43X,*--*,10X,*----*,33X,*I--*,
       2/43X,*DI*,10X,*DI2*,34X,*DI*,/)
    5   FORMAT(I2)
    6   FORMAT(10F8.4)
    7   FORMAT(9X,I2,2(7X,F5.2),5(4X,E9.2))
  100   FORMAT(/1X,100(1H*)/)
        END

        SUBROUTINE DERIV(Y,X,YP,NP)
        DIMENSION Y(20),X(20),YP(20)
        H1=X(2)-X(1)
        YP(1)=(Y(2)-Y(1))/H1
        NPP=NP-1
        DO 10 J=2,NPP
        H1=X(J)-X(J-1)
        H2=X(J+1)-X(J)
        H12= H1+H2
        A=Y(J-1)/(H1*H12)-Y(J)/(H1*H2)+Y(J+1)/(H2*H12)
        B=-(Y(J-1)*(X(J)+X(J+1))/(H1*H12)-Y(J)*(X(J-1)+X(J+1))/
       1(H1*H2)+Y(J+1)*(X(J-1)+X(J))/(H2*H12))
   10   CONTINUE
        UP(NP)=(Y(NP)-Y(NPP))/H2
        RETURN
        END
```

DIODE - SEM(I.C.D.) 1N294

IS = 0.0500 VT = 0.0258

K	V	I	DV/DI	D2V/DI2	DA	R	DV/DI
1	0.00	0.00	0.50E 04	-0.45E 08	0.47E 07	-0.22E 09	0.00E-38
2	0.50	0.00	0.50E 03	-0.45E 08	0.44E 07	-0.23E 09	0.50E-01
3	0.10	0.00	-0.40E 04	-0.45E 08	0.44E 07	-0.23E 09	-0.30E 00
4	0.15	0.20	0.21E 00	0.13E 05	-0.32E 05	0.63E 06	0.42E-01
5	0.20	0.60	0.13E 00	-0.13E 00	0.21E 01	0.44E 01	0.75E-01
6	0.25	1.00	0.11E 00	-0.42E-01	0.18E 01	0.65E 01	0.11E 00
7	0.30	1.60	0.83E-01	-0.28E-01	0.30E 01	0.37E 01	0.13E 00
8	0.35	2.20	0.74E-01	-0.18E-01	0.35E 01	0.34E 01	0.16E 00
9	0.40	3.00	0.57E-01	-0.16E-01	0.58E 01	0.76E 00	0.17E 00
10	0.45	4.00	0.48E-01	-0.58E-02	0.57E 01	0.24E 01	0.19E 00
11	0.50	5.10	0.45E-01	-0.19E-02	0.20E 01	0.36E 01	0.23E 00
12	0.55	6.20	0.44E-01	-0.16E-02	0.25E 01	0.33E 01	0.27E 00
13	0.60	7.40	0.42E-01	-0.20E-02	0.42E 01	0.27E 01	0.31E 00
14	0.65	8.60	0.39E-01	-0.23E-02	0.66E 01	0.19E 01	0.33E 00

A programme and the numerical results for diode IN294 have been given above. One can plot the derivatives versus current and compare it with the results obtained using the system developed. This itself will establish the importance of the present system.